

Superharmonic instability for regularized long-wave models

Jared C. Bronski^{*1}, Vera Mikyong Hur^{†1}, and Samuel Lee Wester^{‡1}

¹Department of Mathematics, University of Illinois at Urbana-Champaign
Urbana, IL 61801, USA

June 1, 2021

Abstract

We examine the spectral stability and instability of periodic traveling waves for regularized long-wave models. Examples include the regularized Boussinesq, Benney–Luke, and Benjamin–Bona–Mahony equations. Of particular interest is a striking new instability phenomenon—spectrum off the imaginary axis extending into infinity. The spectrum of the linearized operator of the generalized Korteweg–de Vries equation, for instance, lies along the imaginary axis outside a bounded set. The spectrum for a regularized long-wave model, by contrast, can vary markedly with the parameters of the periodic traveling waves. We carry out asymptotic spectral analysis to short wavelength perturbations, distinguishing whether the spectrum tends to infinity along the imaginary axis or some curve whose real part is nonzero. We conduct numerical experiments to corroborate our analytical findings.

1 Introduction

The Korteweg–de Vries (KdV) equation [7, 20]

$$u_t + u_x + u_{xxx} + (u^2)_x = 0 \quad (1.1)$$

and the Boussinesq equation [7]

$$u_{tt} - u_{xx} - u_{xxxx} - (u^2)_{xx} = 0 \quad (1.2)$$

are basic mathematical models for small amplitude and relatively long waves in water, under the influence of gravity and possibly surface tension. Here $t \in \mathbb{R}$ is proportional to elapsed time, $x \in \mathbb{R}$ is related to the spatial variable in the direction of wave propagation, and $u(x, t)$ is real valued, describing the fluid surface or a velocity.

There are many variants of (1.1) and (1.2). Under the assumption that $u_t + u_x$ is of smaller order, Benjamin, Bona and Mahony [3] proposed

$$u_t + u_x - u_{xxt} + (u^2)_x = 0$$

^{*}E-mail: bronski@illinois.edu.

[†]E-mail: verahur@math.uiuc.edu. VMH is supported by NSF DMS-2009981.

[‡]E-mail: swester3@illinois.edu

as an alternative to (1.1). Also under the assumption that $u_t \pm u_x$ are of smaller order, the so-called regularized Boussinesq equation*

$$u_{tt} - u_{xx} - u_{xxtt} - (u^2)_{xx} = 0 \quad (1.3)$$

is at least formally equivalent to (1.2) for long waves. Indeed, the dispersion relation of (1.3),

$$\omega^2(k) = \frac{k^2}{1+k^2} = k^2(1 - k^2 + O(k^4)) \quad \text{as } |k| \rightarrow 0,$$

agrees with the dispersion relation of (1.2) up to the order of k^4 when $|k|$ is small, but (1.3) is preferable to (1.2) for short and intermediately long waves because the Cauchy problem for (1.2) is ill-posed.

Another variant is the Benney–Luke equation [4]

$$u_{tt} - u_{xx} + au_{xxxx} - bu_{xxtt} + u_t u_{xx} + 2u_x u_{xt} = 0, \quad (1.4)$$

where[†] $a, b \geq 0$ satisfy $a - b = \text{Bo}^{-1} - \frac{1}{3}$ and Bo^{-1} is the inverse of the Bond number, describing surface tension strength. The dispersion relation of (1.4) is

$$\omega^2(k) = k^2 \frac{1 + ak^2}{1 + bk^2}$$

and remains bounded for all $k \in \mathbb{R}$, provided that $a = 0$ and $b \neq 0$. Also Bona, Chen and Saut [5, 6] proposed a four parameter family of Boussinesq systems

$$\begin{aligned} \eta_t + u_x + au_{xxx} - b\eta_{xxt} + (\eta u)_x &= 0, \\ u_t + \eta_x + c\eta_{xxx} - du_{xxt} + uu_x &= 0, \end{aligned} \quad (1.5)$$

where $a, b, c, d \geq 0$ satisfy $a + b = \frac{1}{2}(\theta^2 - \frac{1}{3})$ and $c + d = \frac{1}{2}(1 - \theta^2)$ for some $\theta \in [0, 1]$. The dispersion relation of (1.5) is

$$\omega^2(k) = k^2 \frac{(1 - ak^2)(1 - ck^2)}{(1 + bk^2)(1 + dk^2)}$$

and remains bounded for all $k \in \mathbb{R}$, provided that a or $c = 0$ while $b, d \neq 0$.

For the generalized KdV equation

$$u_t + u_x + u_{xxx} + (f(u))_x = 0, \quad f \text{ is some nonlinearity}, \quad (1.6)$$

the spectrum of the linearized operator about a periodic traveling wave lies along the imaginary axis outside of a bounded set. See Appendix A for a proof. This is in some sense implicit in many numerical studies of stability and instability. See [8, 10, 11], among others, for analytical studies of stability and instability. We expect that the same holds true for (1.4) and (1.5) so long as $a, c \neq 0$. The proof in Appendix A hinges on the fact that $|\omega(k+1) - \omega(k)| \rightarrow \infty$ as $|k| \rightarrow \infty$, where $\omega(k) = k^3 - k$ is the dispersion relation of (1.6). For regularized long-wave models such as (1.3), and (1.4), where $a = 0$ while $b \neq 0$, and (1.5), where a or $c = 0$ while $b, d \neq 0$, by contrast, $|\omega(k+1) - \omega(k)|$ remains bounded or even vanishes as $|k| \rightarrow \infty$.

Indeed, the asymptotics of the spectrum at infinity of the linearized operator of a regularized long-wave model can vary markedly with the parameters of the periodic traveling waves. Figure 1

*This does not appear explicitly in [7]. But [7, (280)], for instance, after several ‘higher order terms’ drop out, becomes equivalent to what appears in [24].

[†] $a = \frac{1}{6}$ and $b = \frac{1}{2}$ in [4]

provides examples for two periodic traveling waves of (1.3), for which only one of the parameters differs less than 4%. On the left, the spectrum lies along the imaginary axis outside of a bounded set. On the right, on the other hand, the spectrum tends towards infinity along the dashed lines whose real part is nonzero. Indeed, the periodic traveling wave is spectrally unstable to arbitrarily short wavelength perturbations, the opposite to modulational instability to arbitrarily long wavelength perturbations. The aim here is to explain such striking and new instability for (1.3), and (1.4), where $a = 0$ while $b \neq 0$, and (1.5), where $a, c = 0$ while $b, d \neq 0$. Modulational instability will be addressed in a companion article [9].

In Section 2 we set forth asymptotic spectral analysis to short wavelength perturbations for (1.3), demonstrating that: if an associated Hill's differential equation (see (2.20)) is elliptic (in a band), depending on the parameters of the periodic traveling wave, then the spectrum tends to infinity along the imaginary axis. If (2.20) is hyperbolic (in a gap), on the other hand, then the spectrum tends to infinity along a line whose real part is nonzero. Actually, (2.20) is a three-gap Lamé equation, whose band edges can be found in closed form, enabling us to classify the spectrum at infinity for all periodic traveling waves. We compute the spectrum numerically to corroborate the analytical predictions.

In Section 3 we turn our attention to (1.4), where $a = 0$ and, for simplicity of notation, $b = 1$. The associated Lamé equation (see (3.16)) is no longer explicitly solvable. Nevertheless we can compute the band edges numerically, distinguishing whether the spectrum tends to infinity along the imaginary axis or some line whose real part is nonzero.

Last but not least, in Section 4, we turn to (1.5), where $a = c = 0$ and[‡] $b = d = \frac{1}{6}$, and establish that: if the mean of $1 + \eta$ over the period is negative, depending on the parameters of the periodic traveling wave, then the spectrum tends to infinity along some curve whose real part is $O(k^{-1})$ for $|k| \gg 1$, that is, short wavelength perturbations. Numerical results are in excellent agreement with analytical ones.

2 The regularized Boussinesq equation

We begin by rewriting (1.3) as

$$u_t = (1 - \partial_x^2)^{-1} v_x \quad \text{and} \quad v_t = (u + u^2)_x$$

or, equivalently [17],

$$\begin{pmatrix} u \\ v \end{pmatrix}_t = \begin{pmatrix} 0 & \partial_x \\ \partial_x & 0 \end{pmatrix} \begin{pmatrix} u + u^2 \\ (1 - \partial_x^2)^{-1} v \end{pmatrix}. \quad (2.1)$$

Throughout the section we employ the notation $\mathbf{u} = \begin{pmatrix} u \\ v \end{pmatrix}$. We remark that (2.1) is in the Hamiltonian form

$$\mathbf{u}_t = J\delta H(\mathbf{u}),$$

where $J = \begin{pmatrix} 0 & \partial_x \\ \partial_x & 0 \end{pmatrix}$ is the symplectic form,

$$H(\mathbf{u}) = \int \left(\frac{1}{2} u^2 + \frac{1}{3} u^3 + \frac{1}{2} v (1 - \partial_x^2)^{-1} v \right) dx$$

[‡]for convenience and to better corresponds to earlier works [12, 13]

is the Hamiltonian, and δ denotes variational differentiation. In addition to H , (2.1) has three conserved quantities

$$\begin{aligned} P(\mathbf{u}) &= \int uv \, dx && \text{(momentum),} \\ M_1(\mathbf{u}) &= \int u \, dx \quad \text{and} \quad M_2(\mathbf{u}) = \int v \, dx && \text{(masses).} \end{aligned}$$

2.1 Parametrization of periodic traveling waves

A traveling wave of (2.1) takes the form $\mathbf{u}(x - ct - x_0)$, where $c \neq 0, \in \mathbb{R}$ is the wave speed and $x_0 \in \mathbb{R}$ the spatial translate, and it arises as a critical point of the ‘augmented Hamiltonian’

$$H_{\text{aug}} = H + cP + b_1M_1 + b_2M_2$$

for some $b_1, b_2 \in \mathbb{R}$. That is,

$$\delta H_{\text{aug}}(\mathbf{u}) = \begin{pmatrix} u + u^2 + cv + b_1 \\ (1 - \partial_x^2)^{-1}v + cu + b_2 \end{pmatrix} = \mathbf{0}. \quad (2.2)$$

Eliminating v from (2.2), we arrive at

$$c^2u'' + (1 - c^2)u + u^2 + b_1 - b_2c = 0. \quad (2.3)$$

Here and elsewhere, the prime denotes ordinary differentiation. Multiplying (2.3) through by u' and integrating, moreover,

$$\frac{1}{2}c^2(u')^2 = E - V(u; c, b_1, b_2), \quad V(u; c, b_1, b_2) = \frac{1}{3}u^3 + \frac{1}{2}(1 - c^2)u^2 + (b_1 - b_2c)u, \quad (2.4)$$

for some $E \in \mathbb{R}$. One can perform phase plane analysis for the existence of non-constant periodic solutions of (2.4) and, hence, non-constant periodic traveling waves of (2.1), depending on $c, b_1, b_2, E \in \mathbb{R}$, or depending on $\alpha, \beta, \gamma \in \mathbb{R}$ such that $\alpha < \beta < \gamma$, the roots of the cubic polynomial $E - V(u; c, b_1, b_2)$, provided that they exist. A straightforward calculation reveals that

$$E = \frac{1}{3}\alpha\beta\gamma, \quad b_1 - b_2c = \frac{1}{3}(\alpha\beta + \beta\gamma + \alpha\gamma) \quad \text{and} \quad c^2 - 1 = \frac{2}{3}(\alpha + \beta + \gamma). \quad (2.5)$$

Since $c \neq 0$, $\alpha + \beta + \gamma > -\frac{3}{2}$ must hold true. Let

$$\Delta = \left\{ (\alpha, \beta, \gamma) \in \mathbb{R}^3 : \alpha < \beta < \gamma \quad \text{and} \quad \alpha + \beta + \gamma > -\frac{3}{2} \right\}. \quad (2.6)$$

Figure 4 shows Δ in the (α, β) plane when $\gamma = 1$.

A traveling wave of (2.1) depends additionally on x_0 . On the other hand, (2.1) remains invariant under the translation of the x axis, whereby we can mod out x_0 , requiring $\mathbf{u}'(0) = \mathbf{0}$, that is, \mathbf{u} is even.

Actually, periodic solutions of (2.3) can be found in closed form in terms of the Jacobi elliptic functions. Recall that $y(x) = \text{sn}(x, \sqrt{m})$ is a solution of

$$y'' + (1 + m)y = 2my^3,$$

where $m \in (0, 1)$ is the elliptic parameter, and $z(x) = \text{sn}^2(x, \sqrt{m})$ is a solution of

$$z'' + 4(1 + m)z = 2 + 6mz^2.$$

Throughout we work with the elliptic parameter rather than the elliptic modulus k , where $m = k^2$. Let $(\alpha, \beta, \gamma) \in \Delta$ and our task is to solve (2.3) or, equivalently,

$$u'' - \frac{2(\alpha + \beta + \gamma)}{2(\alpha + \beta + \gamma) + 3}u + \frac{3}{2(\alpha + \beta + \gamma) + 3}u^2 + \frac{\alpha\beta + \beta\gamma + \alpha\gamma}{2(\alpha + \beta + \gamma) + 3} = 0 \quad (2.7)$$

by (2.5), subject to, say,

$$u(0) = \gamma \quad \text{and} \quad u'(0) = 0.$$

Trying

$$u(x) = \gamma - (\gamma - \beta) \operatorname{sn}^2(ax, \sqrt{m}), \quad (2.8)$$

after some algebra we find

$$m = \frac{\gamma - \beta}{\gamma - \alpha} \quad \text{and} \quad a = \sqrt{\frac{\gamma - \alpha}{4(\alpha + \beta + \gamma) + 6}}. \quad (2.9)$$

Clearly, $0 < m < 1$ and $a > 0$. The period of (2.8) is

$$T = \frac{2K(\sqrt{m})}{a}, \quad (2.10)$$

where

$$K(\sqrt{m}) = \int_0^1 \frac{ds}{\sqrt{(1-s^2)(1-ms^2)}}$$

is the complete elliptic integral of the first kind.

To summarize, whenever $(\alpha, \beta, \gamma) \in \Delta$, (2.8) gives a periodic traveling wave of (2.1), depending on α, β, γ by (2.9), where v is in (2.2).

Remark. More generally, consider

$$u_{tt} - u_{xx} - u_{xxtt} - f(u)_{xx} = 0, \quad f \text{ is some nonlinearity.} \quad (2.11)$$

When $f(u) = u^2$, (2.11) becomes (1.3). Proceeding as above, one can deduce that a traveling wave of (2.11) satisfies

$$\frac{1}{2}c^2(u')^2 = E - V(u; c, b_1, b_2), \quad V(u, c, b_1, b_2) = F(u) + \frac{1}{2}(1 - c^2)u^2 + (b_1 - b_2c)u, \quad (2.12)$$

for some $c \neq 0, \in \mathbb{R}$ for some $b_1, b_2, E \in \mathbb{R}$, where $F' = f$. If $E - V(u; c, b_1, b_2)$ has simple roots u_{\pm} , depending on c, b_1, b_2, E , such that $u_- < u_+$ and if $E - V(u; c, b_1, b_2) > 0$ for $u \in (u_-, u_+)$ then (2.12) has a non-constant periodic solution, whose period is

$$T = \sqrt{2} \int_{u_-}^{u_+} \frac{c \, du}{\sqrt{E - V(u; c, b_1, b_2)}} = \frac{\sqrt{2}}{2} \oint_{\Gamma} \frac{c \, du}{\sqrt{E - V(u; c, b_1, b_2)}},$$

where Γ is a Jordan curve in the complex u plane containing the interval $[u_-, u_+]$ in the interior region. One can treat the contour integration at the branch points in the usual way.

All of what follows would succeed with (2.11) mutatis mutandis. One does not expect that periodic traveling waves of (2.11) can be found in closed form, except for few nonlinearities, but their parametrization by c, b_1, b_2, E suffices. Here we focus our attention to $f(u) = u^2$, nevertheless, because such a nonlinearity is characteristic of many wave phenomena and, moreover, leads to simple analytic formulae.

2.2 Asymptotic spectral analysis to short wavelength perturbations

Let $(\alpha, \beta, \gamma) \in \Delta$ (see (2.6)) and \mathbf{u} denotes a periodic traveling wave of (2.1) (see (2.2), (2.8), (2.9)), c the wave speed (see the third equation of (2.5)) and T the period (see (2.10)), depending on α, β, γ . Linearizing (2.1) about \mathbf{u} in the frame of reference moving at the speed c , we arrive at

$$\phi_t = J\delta^2 H_{\text{aug}}(\mathbf{u})\phi = \begin{pmatrix} 0 & \partial_x \\ \partial_x & 0 \end{pmatrix} \begin{pmatrix} 1 + 2u & c \\ c & (1 - \partial_x^2)^{-1} \end{pmatrix} \phi.$$

Seeking a solution of the form $\phi(x, t) = e^{\lambda t} \phi(x)$, $\lambda \in \mathbb{C}$, we arrive at

$$\lambda \phi = \begin{pmatrix} c\partial_x & \partial_x(1 - \partial_x^2)^{-1} \\ \partial_x(1 + 2u) & c\partial_x \end{pmatrix} \phi =: \mathbf{L}(\mathbf{u})\phi, \quad (2.13)$$

where $\mathbf{L}(\mathbf{u}) : H^1(\mathbb{R}) \times H^1(\mathbb{R}) \subset L^2(\mathbb{R}) \times L^2(\mathbb{R}) \rightarrow L^2(\mathbb{R}) \times L^2(\mathbb{R})$. We say that \mathbf{u} is spectrally stable if the spectrum of $\mathbf{L}(\mathbf{u})$ lies in the left half plane of \mathbb{C} , where $\text{Re}(\lambda) \leq 0$, and spectrally unstable otherwise. The spectrum of $\mathbf{L}(\mathbf{u})$ is symmetric about the real and imaginary axes because (2.1) is in the Hamiltonian form, whereby \mathbf{u} is spectrally stable if and only if the spectrum of $\mathbf{L}(\mathbf{u})$ is contained in the imaginary axis.

Since $\mathbf{L}(\mathbf{u})$ is T periodic in the x variable, Floquet theory (see [14, Theorem 2.95], for instance) implies that λ is in the spectrum if and only if (2.13) has a nontrivial bounded solution such that

$$\phi(x + T) = e^{\frac{2\pi i k x}{T}} \phi(x) \quad \text{for some } k \in \mathbb{R}.$$

One can write $k = [k] + \tau$, where $[k] \in \mathbb{Z}$, and $\tau \in (-\frac{1}{2}, \frac{1}{2}]$ is the Floquet exponent. We focus our attention to superharmonic and, particularly, short wavelength perturbations, for which $|k| \gg 1$. Indeed, our numerical experiments (see Figure 1, for instance) show a striking and new instability phenomenon—spectrum off the imaginary axis extending all the way to $\pm i\infty$ —for some \mathbf{u} , that is, for some α, β, γ . The aim here is to explain such instability. Subharmonic and, particularly, long wavelength perturbations, for which $|k| \neq 0, \ll 1$, will be addressed in [9].

Since

$$\mathbf{L}(\mathbf{u})e^{\frac{2\pi i k x}{T}} = \begin{pmatrix} O(k) & O(k^{-1}) \\ O(k) & O(k) \end{pmatrix} \quad \text{as } |k| \rightarrow \infty,$$

we make the ansatz

$$\lambda = \lambda^{(1)}k + \lambda^{(0)} + \lambda^{(-1)}k^{-1} + \dots \quad \text{and} \quad \phi(x) = e^{\frac{2\pi i k x}{T}} (\phi^{(0)}(x) + \phi^{(-1)}(x)k^{-1} + \phi^{(-2)}(x)k^{-2} + \dots) \quad (2.14)$$

as $|k| \rightarrow \infty$ for some $\lambda^{(1)}, \lambda^{(0)}, \lambda^{(-1)}, \dots \in \mathbb{C}$ for some $\phi^{(0)}, \phi^{(-1)}, \phi^{(-2)}, \dots \in L^\infty(\mathbb{R}) \times L^\infty(\mathbb{R})$, to be determined. Substituting (2.14) into (2.13),

$$\begin{aligned} & (\lambda^{(1)}k + \lambda^{(0)} + \lambda^{(-1)}k^{-1} + \dots)(\phi^{(0)} + \phi^{(-1)}k^{-1} + \phi^{(-2)}k^{-2} + \dots) \\ &= \begin{pmatrix} c\left(\frac{2\pi i k}{T} + \partial_x\right) & \left(\frac{2\pi i k}{T} + \partial_x\right)\left(1 - \left(\frac{2\pi i k}{T} + \partial_x\right)^2\right)^{-1} \\ \left(\frac{2\pi i k}{T} + \partial_x\right)(1 + 2u) & c\left(\frac{2\pi i k}{T} + \partial_x\right) \end{pmatrix} (\phi^{(0)} + \phi^{(-1)}k^{-1} + \phi^{(-2)}k^{-2} + \dots) \\ &=: (\mathbf{L}^{(1)}k + \mathbf{L}^{(0)} + \mathbf{L}^{(-1)}k^{-1} + \dots)(\phi^{(0)} + \phi^{(-1)}k^{-1} + \phi^{(-2)}k^{-2} + \dots) \end{aligned}$$

as $|k| \rightarrow \infty$, where

$$\mathbf{L}^{(1)} = \begin{pmatrix} \frac{2\pi i c}{T} & 0 \\ \frac{2\pi i c}{T}(1 + 2u) & \frac{2\pi i c}{T} \end{pmatrix}, \quad \mathbf{L}^{(0)} = \begin{pmatrix} c\partial_x & 0 \\ \partial_x(1 + 2u) & c\partial_x \end{pmatrix} \quad \text{and} \quad \mathbf{L}^{(-1)} = \begin{pmatrix} 0 & -\frac{T}{2\pi i} \\ 0 & 0 \end{pmatrix}.$$

At the order of k , we gather

$$\lambda^{(1)}\phi^{(0)} = \mathbf{L}^{(1)}\phi^{(0)} = \begin{pmatrix} \frac{2\pi ic}{T} & 0 \\ \frac{2\pi i}{T}(1+2u) & \frac{2\pi ic}{T} \end{pmatrix} \phi^{(0)},$$

whence

$$\lambda^{(1)} = \frac{2\pi ic}{T} \quad \text{and} \quad \phi^{(0)} = \begin{pmatrix} 0 \\ \phi_2^{(0)} \end{pmatrix}, \quad (2.15)$$

where $\phi_2^{(0)}$ is bounded and otherwise arbitrary.

At the order of 1, we gather

$$\begin{aligned} \frac{2\pi ic}{T} \begin{pmatrix} \phi_1^{(-1)} \\ \phi_2^{(-1)} \end{pmatrix} + \lambda^{(0)} \begin{pmatrix} 0 \\ \phi_2^{(0)} \end{pmatrix} &= \lambda^{(1)}\phi^{(-1)} + \lambda^{(0)}\phi^{(0)} \\ &= \mathbf{L}^{(1)}\phi^{(-1)} + \mathbf{L}^{(0)}\phi^{(0)} \\ &= \begin{pmatrix} \frac{2\pi ic}{T} & 0 \\ \frac{2\pi i}{T}(1+2u) & \frac{2\pi ic}{T} \end{pmatrix} \begin{pmatrix} \phi_1^{(-1)} \\ \phi_2^{(-1)} \end{pmatrix} + \begin{pmatrix} c\partial_x & 0 \\ \partial_x(1+2u) & c\partial_x \end{pmatrix} \begin{pmatrix} 0 \\ \phi_2^{(0)} \end{pmatrix}, \end{aligned}$$

whence

$$\frac{2\pi i}{T}(1+2u)\phi_1^{(-1)} = (\lambda^{(0)} - c\partial_x)\phi_2^{(0)}. \quad (2.16)$$

At the order of k^{-1} , similarly,

$$\begin{aligned} \begin{pmatrix} 0 & 0 \\ \frac{2\pi i}{T}(1+2u) & 0 \end{pmatrix} \phi^{(-2)} &= (\mathbf{L}^{(1)} - \lambda^{(1)})\phi^{(-2)} \\ &= -(\mathbf{L}^{(0)} - \lambda^{(0)})\phi^{(-1)} - (\mathbf{L}^{(-1)} - \lambda^{(-1)})\phi^{(0)} \\ &= \begin{pmatrix} (\lambda^{(0)} - c\partial_x)\phi_1^{(-1)} + \frac{T}{2\pi i}\phi_2^{(0)} \\ -\partial_x((1+2u)\phi_1^{(-1)}) + (\lambda^{(0)} - c\partial_x)\phi_2^{(-1)} - \lambda^{(-1)}\phi_2^{(0)} \end{pmatrix}, \end{aligned}$$

which is solvable by the Fredholm alternative, provided that

$$(\lambda^{(0)} - c\partial_x)\phi_1^{(-1)} + \frac{T}{2\pi i}\phi_2^{(0)} = 0. \quad (2.17)$$

We can write (2.16) and (2.17) as

$$\begin{pmatrix} \frac{2\pi i}{T}(\lambda^{(0)} - c\partial_x) & 1 \\ -\frac{2\pi i}{T}(1+2u) & (\lambda^{(0)} - c\partial_x) \end{pmatrix} \begin{pmatrix} \phi_1^{(-1)} \\ \phi_2^{(0)} \end{pmatrix} = \mathbf{0},$$

and rewrite more conveniently as

$$\left(\lambda^{(0)} \mathbf{1} - \begin{pmatrix} c\partial_x & -1 \\ 1+2u & c\partial_x \end{pmatrix} \right) \begin{pmatrix} \frac{2\pi i}{T}\phi_1^{(-1)} \\ \phi_2^{(0)} \end{pmatrix} = \mathbf{0},$$

where $\mathbf{1}$ denotes the identity operator, or as a quadratic pencil as

$$((\lambda^{(0)} - c\partial_x)^2 + 1 + 2u)\phi = 0. \quad (2.18)$$

Our task is to distinguish whether $\text{Re}(\lambda^{(0)}) = 0$ or not, for which (2.18) has a nontrivial bounded solution. After the change of variables

$$\phi = ye^{-\lambda^{(0)}x}, \quad (2.19)$$

(2.18) becomes the Hill's differential equation

$$c^2y'' + (1 + 2u)y = 0. \quad (2.20)$$

Recall [15, 21] that solutions of (2.20) can be classified as:

- **Elliptic (band).** (2.20) has two linearly independent solutions y_1 and y_2 , say, such that $y_1(x + T) = e^{i\sigma T}y_1(x)$ and $y_2(x + T) = e^{-i\sigma T}y_2(x)$ for some $\sigma \in \mathbb{R}$;
- **Parabolic (band edge).** (2.20) has two linearly independent solutions y_1 and $xy_1 + y_2$ such that $y_1(x + T) = y_1(x)$ and $y_2(x + T) = y_2(x)$; and
- **Hyperbolic (gap).** (2.20) has two linearly independent solutions y_1 and y_2 such that

$$y_1(x + T) = e^{\sigma T}y_1(x) \quad \text{and} \quad y_2(x + T) = e^{-\sigma T}y_2(x) \quad \text{for some } \sigma > 0, \quad (2.21)$$

the Lyapunov exponent. A degenerate band edge (closed gap) is included in a band for convenience. Therefore, $\lambda^{(0)}$ and bounded solutions of (2.18) can be classified.

Lemma 1. *If (2.20) is elliptic (in a band) then (2.18) has a bounded solution if and only if $\text{Re}(\lambda^{(0)}) = 0$, in which case all solutions are bounded. If (2.20) is parabolic (band edge) then (2.18) has a bounded solution if and only if $\text{Re}(\lambda^{(0)}) = 0$, in which case there is only one linearly independent bounded solution.*

If (2.20) is hyperbolic (in a gap), on the other hand, then (2.18) has a bounded solution if and only if $\text{Re}(\lambda^{(0)}) = \pm\sigma$, where $\sigma > 0$ is the Lyapunov exponent of (2.20) (see (2.21)), in which case there is only one linearly independent bounded solution for each value of $\text{Re}(\lambda^{(0)})$.

Proof. If $\text{Re}(\lambda^{(0)}) = 0$ then (2.19) maps from bounded solutions of (2.20) to bounded solutions of (2.18). Otherwise, (2.19) can map to bounded solutions of (2.18), provided that $\text{Re}(\lambda^{(0)}) = \pm\sigma$. ■

We summarize our conclusion.

Theorem 2. *Let $(\alpha, \beta, \gamma) \in \Delta$ and \mathbf{u} denotes a periodic traveling wave of (2.1), c the wave speed and T the period, depending on α, β, γ . If (2.20) is elliptic (in a band) then the spectrum of (2.13) tends to infinity along the imaginary axis. If (2.20) is hyperbolic (in a gap), on the other hand, then the spectrum tends to infinity along $\pm\sigma + i\mathbb{R}$, where $\sigma > 0$ is the Lyapunov exponent of (2.20) (see (2.21)).*

Consequently, when (2.20) is in a gap, the periodic traveling wave is spectrally unstable to arbitrarily short wavelength perturbations, in marked contrast to modulational instability to arbitrarily long wavelength perturbations. Note that, while we cannot establish stability in this way having (2.20) hyperbolic is a sufficient condition for instability.

We remark that $\text{Im}(\lambda^{(0)})$ does not occupy a crucial role. This is because $\lambda \sim \lambda^{(1)}k = \frac{2\pi i ck}{T}$ as $|k| \rightarrow \infty$ to leading order (see (2.14) and (2.15)) and $\text{Im}(\lambda^{(0)})$ serves to translate such—otherwise arbitrary—spectrum along the imaginary axis. Indeed, we can take $\text{Im}(\lambda^{(0)}) = 0$ without loss of generality.

Moreover, the Lyapunov exponent of (2.20) can be found in terms of the monodromy matrix. Let $(\alpha, \beta, \gamma) \in \Delta$, and y_1 and y_2 denote two solutions of (2.20) such that

$$y_1(0) = 1, \quad y_1'(0) = 0 \quad \text{and} \quad y_2(0) = 0, \quad y_2'(0) = 1.$$

Let

$$\mathbf{Y} = \begin{pmatrix} y_1(T) & y_2(T) \\ y_1'(T) & y_2'(T) \end{pmatrix}$$

be the monodromy matrix of (2.20), depending on α, β, γ . Notice that $\det(\mathbf{Y}) = 1$. If (2.20) is in a gap, that is, $|\operatorname{tr}(\mathbf{Y})| > 2$, then \mathbf{Y} has an eigenvalue of modulus > 1 , and

$$\sigma = \frac{\log(|\mu|)}{T}, \quad \mu \text{ is the eigenvalue of } \mathbf{Y} \text{ such that } |\mu| > 1.$$

Correspondingly, the spectrum of (2.13) tends to infinity along $\lambda^{(0)} + i\mathbb{R}$, where

$$\lambda^{(0)} = \pm \frac{\log(|\mu|)}{T} \pmod{\frac{2\pi ic}{T}}.$$

The assumption that $\operatorname{Re}(\lambda^{(0)}) \neq 0$ guarantees that $|\mu| \neq 1$, which in turn guarantees that (2.19) is valid. That means, (2.20) is not in a band or band edge and, particularly, $\operatorname{tr}(\mathbf{Y}) \neq \pm 2$, whereby solutions of (2.20) do not exhibit secular growth.

2.3 Numerical experiments corroborating analytical predictions

We discuss a Fourier spectral method for computing the spectrum of (2.13) numerically. For $\tau \in (-\frac{1}{2}, \frac{1}{2}]$, the Floquet exponent, let

$$\phi(x) = e^{\frac{2\pi i \tau x}{T}} \psi(x), \quad \psi(x+T) = \psi(x),$$

whence

$$\psi(x) = \sum_{k \in \mathbb{Z}} \hat{\psi}_k e^{\frac{2\pi i k x}{T}}, \quad \hat{\psi}_k \text{ are the Fourier coefficients.}$$

We rewrite (2.13) as

$$\lambda \psi = \begin{pmatrix} c \left(\frac{2\pi i \tau}{T} + \partial_x \right) & \left(\frac{2\pi i \tau}{T} + \partial_x \right) \left(1 - \left(\frac{2\pi i \tau}{T} + \partial_x \right)^2 \right)^{-1} \\ \left(\frac{2\pi i \tau}{T} + \partial_x \right) (1 + 2u) & c \left(\frac{2\pi i \tau}{T} + \partial_x \right) \end{pmatrix} \psi, \quad (2.22)$$

where

$$u(x) = \sum_{k \in \mathbb{Z}} \hat{u}_k e^{\frac{2\pi i k x}{T}}, \quad \hat{u}_k \text{ are the Fourier coefficients,}$$

c and T depend on $(\alpha, \beta, \gamma) \in \Delta$. We then make the Fourier collocation projection of (2.22) to the subspace of $L^2(-\frac{T}{2}, \frac{T}{2}) \times L^2(-\frac{T}{2}, \frac{T}{2})$, for which $k = -N_k, -N_k + 1, \dots, N_k$. For each τ , we run the native eigenvalue solver in Mathematica for the resulting $(4N_k + 2) \times (4N_k + 2)$ matrix, made up of sums and products of diagonal and Toeplitz matrices, representing differential operators and multiplications by periodic functions, respectively. In all of our numerical experiments, $N_k = 100$ and we take a 200-points discretization of $\tau \in (-\frac{1}{2}, \frac{1}{2}]$.

We exploit an analytic formula for the Fourier series of a Jacobi elliptic function [19]

$$\operatorname{sn}^2(x, \sqrt{m}) = \frac{K(\sqrt{m}) - E(\sqrt{m})}{mK(\sqrt{m})} - \frac{2\pi^2}{mK^2(\sqrt{m})} \sum_{k=1}^{\infty} \frac{kq^k}{1 - q^{2k}} \cos\left(\frac{\pi k x}{K(\sqrt{m})}\right),$$

to evaluate \hat{u}_k numerically, where $K(\sqrt{m})$ and $E(\sqrt{m})$ denote the complete elliptic integrals of the first and second kinds, $m \in (0, 1)$ is the elliptic parameter, and $q = e^{-\frac{\pi K(\sqrt{1-m})}{K(\sqrt{m})}}$. As an additional numerical check we integrate (2.3) (or (2.7)) numerically and approximate the Fourier coefficients by numerical quadrature. The results are in excellent agreement.

When (2.20) is in a gap, we also integrate (2.20) numerically to find the eigenvalues of the monodromy matrix. They determine the spectrum of (2.13) off the imaginary axis at infinity.

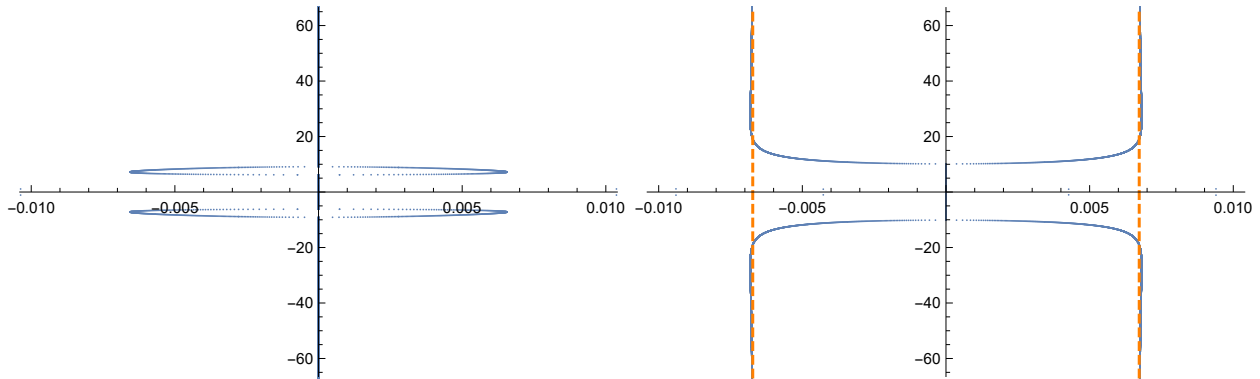


Figure 1: The numerically computed spectrum of (2.13), where u, c, T depend on α, β, γ . On the left, $\alpha = -0.7600, \beta = -0.006403, \gamma = 1$, for which (2.20) is in a band. Notice modulational instability near $0 \in \mathbb{C}$, although it is hard to distinguish, and finite wavelength instability near $\pm 7.5i$. The spectrum lies along the imaginary axis otherwise. On the right, $\alpha = -0.7872, \beta = -0.006403, \gamma = 1$, for which (2.20) is in a gap. The spectrum tends towards infinity along the dashed lines $\pm\sigma + i\mathbb{R}$, where $\sigma \approx 0.006726$. We report modulational instability near $0 \in \mathbb{C}$.

Figure 1 provides two examples of the numerically computed spectrum of (2.13). The periodic traveling waves are close together in Δ (see also Figure 4)—indeed, only the value of α differs slightly—and yet they exhibit a dramatic difference in the spectrum at $\pm i\infty$. In the left panel, for which (2.20) is elliptic (in a band), the spectrum lies apparently along the imaginary axis outside of some bounded set. In the right panel, on the other hand, the spectrum tends towards infinity along $\pm\sigma + i\mathbb{R}$, where $\sigma \approx 0.006726$, and σ agrees well with $\frac{\log(|\mu|)}{T}$, where μ is numerically computed eigenvalue of the monodromy matrix of (2.20) such that $|\mu| > 1$. Therefore the numerical result corroborates Theorem 2. There is a modulational instability to long wavelength perturbations near $0 \in \mathbb{C}$ in both panels, although it is hard to distinguish at this scale. Also there is spectral instability to finite wavelength perturbations away from $0 \in \mathbb{C}$ in the left panel.

In the left panel of Figure 2, for which (2.20) is in a gap—the second gap of the associated Lamé equation (see Section 2.4)—the numerically computed spectrum tends towards infinity along $\pm\sigma + i\mathbb{R}$, where $\sigma \approx 0.455$, far greater than the right panel of Figure 1, and σ agrees well with $\frac{\log(|\mu|)}{T}$, where μ is the numerically computed eigenvalue of the monodromy matrix of (2.20) such that $|\mu| > 1$. See also Figure 3 for modulational instability.

Last but not least, in the right panel of Figure 2, for which (2.20) is in a band—indeed, (2.23) is in the third band (see Section 2.4)—the numerical result is consistent with Theorem 2 as the spectrum tends towards infinity along the imaginary axis. The greatest real part of the numerically computed spectrum is of the order of 10^{-8} , suggesting spectral stability.

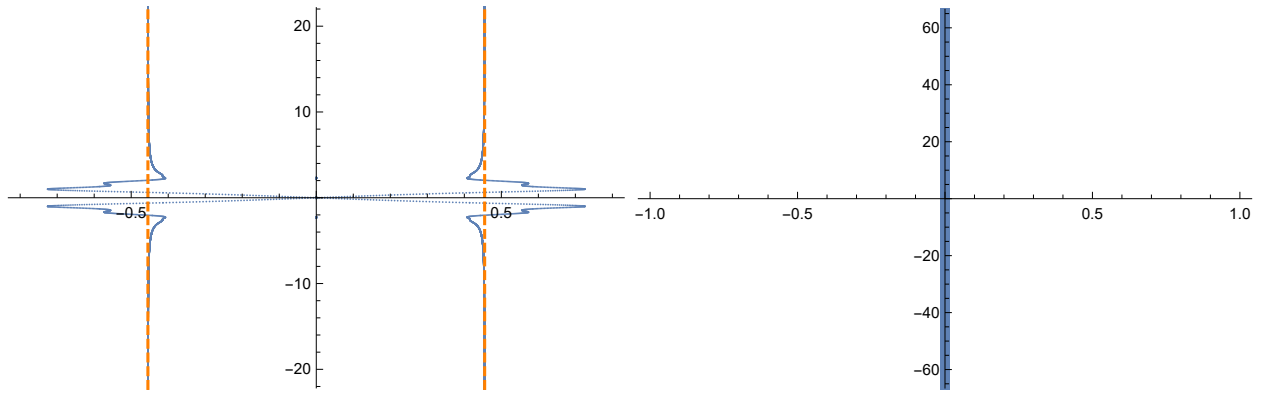


Figure 2: The spectrum of (2.13). On the left, $\alpha = -1.246$, $\beta = -1.149$, $\gamma = 1$, for which (2.20) is in a gap. The spectrum tends towards infinity along the dashed lines $\pm\sigma + i\mathbb{R}$, where $\sigma \approx 0.455$. Notice modulational instability near $0 \in \mathbb{C}$ (see also Figure 3). On the right, $\alpha = -2.034$, $\beta = 0.7131$, $\gamma = 1$, for which (2.20) is in a band. The spectrum lies along the imaginary axis, suggesting spectral stability.

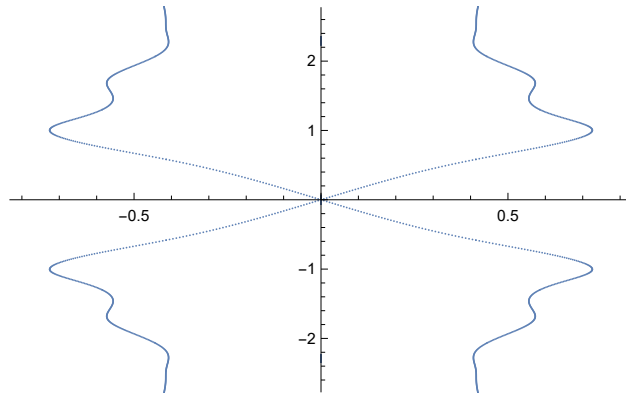


Figure 3: $\alpha = -1.246$, $\beta = -1.149$, $\gamma = 1$ (see the left panel of Figure 2), and the spectrum of (2.13) near $0 \in \mathbb{C}$ for modulational instability.

2.4 Analytic formulae classifying the spectrum at infinity

We can rewrite (2.8) as

$$u(x) = \gamma - 6ma^2c^2 \operatorname{sn}^2(ax, \sqrt{m}),$$

where m and a are in (2.9), and c is in the third equation of (2.5), whence (2.20) as

$$y'' + \left(\frac{2\gamma + 1}{c^2} - 12ma^2 \operatorname{sn}^2(ax, \sqrt{m}) \right) y = 0.$$

After the change of variables $x \mapsto \frac{x}{a}$, we arrive at the Lamé equation (in the Jacobi form) [2]

$$y'' + (\ell - 3(3+1)m \operatorname{sn}^2(x, \sqrt{m}))y = 0, \quad (2.23a)$$

where

$$\ell = \frac{6(2\gamma + 1)}{\gamma - \alpha} = 4 + 4m + \frac{1}{a^2} \quad (2.23b)$$

by (2.5) and (2.9).

Recall [2, 18] that (2.23a) has exactly three finite (open) gaps plus one semi-infinite gap, whence four disjoint bands, whose band edges can be found in closed form in terms of the roots of some polynomials. Specifically, let $\{\ell_j^P\}_{j=1}^\infty$ denote the periodic eigenvalues of (2.23a) and $\{\ell_j^A\}_{j=1}^\infty$ the anti-periodic eigenvalues, respectively, such that

$$-\infty < \ell_1^P < \ell_1^A < \ell_2^A < \ell_2^P < \ell_3^P < \ell_3^A < \ell_4^A \leq \dots,$$

and

$$\begin{aligned} \ell_1^P &= 2 + 5m - 2\theta_1, & \ell_2^P &= 4 + 4m, & \ell_3^P &= 2 + 5m + 2\theta_1, \\ \ell_1^A &= 5 + 2m - \theta_2, & \ell_2^A &= 5 + 5m - 2\theta_3, & \ell_3^A &= 5 + 2m + 2\theta_2, & \ell_4^A &= 5 + 5m + 2\theta_3, \end{aligned}$$

where

$$\theta_1 = \sqrt{1 - m + 4m^2}, \quad \theta_2 = \sqrt{4 - m + m^2}, \quad \theta_3 = \sqrt{4 - 7m + 4m^2},$$

and $\ell_j^A = \ell_j^P = \ell_{j+1}^P = \ell_{j+1}^A$ for $j \geq 4, \in \mathbb{Z}$. The bands of (2.23a) consist of

$$(\ell_1^P, \ell_1^A), \quad (\ell_2^A, \ell_2^P), \quad (\ell_3^P, \ell_3^A) \quad \text{and} \quad (\ell_4^A, \infty), \quad (2.24)$$

and the gaps consist of

$$(-\infty, \ell_1^P), \quad (\ell_1^A, \ell_2^A), \quad (\ell_2^P, \ell_3^P) \quad \text{and} \quad (\ell_3^A, \ell_4^A). \quad (2.25)$$

We refer to $(-\infty, \ell_1^P)$ as the zeroth gap for convenience.

If (2.23) lies in a band, that is, (2.23b) is in (2.24), then the spectrum of (2.13) tends to infinity along the imaginary axis. If (2.23) is in a gap, that is, (2.25), on the other hand, then the spectrum tends to infinity along $\pm\sigma + i\mathbb{R}$ for some $\sigma > 0$. Therefore we achieve analytic formulae, depending on m and a , whence depending on α, β, γ by (2.9), which classify the spectrum of (2.13) at infinity.

Figure 4 shows bands and gaps of (2.23) in the (α, β) plane when $\gamma = 1$. Notice that not all bands and gaps are present in Δ . Specifically, the zeroth and first gaps, and the first and second bands are not present. But when a band or a gap is present in Δ , it is entirely contained in Δ . For a proof, we observe that:

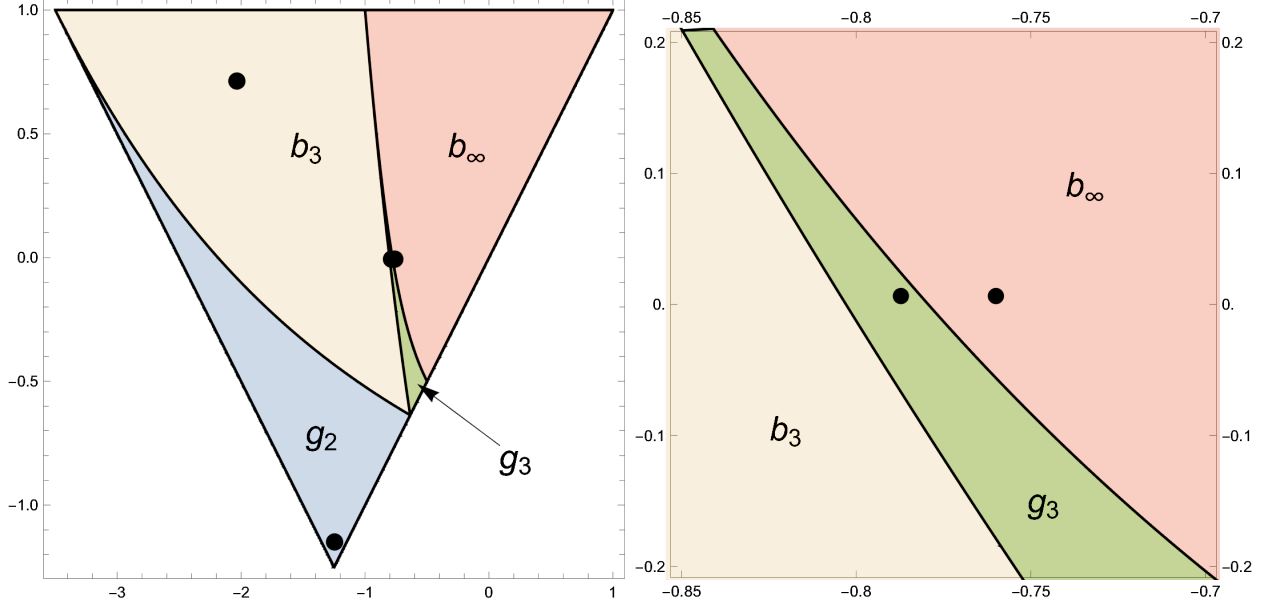


Figure 4: Δ in the (α, β) plane when $\gamma = 1$: g_2 denotes the region, for which (2.23) is in the second gap, that is, (2.23b) is in (ℓ_2^P, ℓ_3^P) , and g_3 the third gap (ℓ_3^A, ℓ_4^A) . Also b_3 denotes the region, for which (2.23) is in the third band, that is, (ℓ_3^P, ℓ_3^A) , and b_∞ the band (ℓ_4^A, ∞) . The bullet points correspond to the values of (α, β) for Figures 1 and 2. On the right is a close-up of the values of (α, β) for Figure 1.

- The top edge of Δ , where $\beta = 1$, corresponds to $m = 0$, and the right edge, where $\alpha = \beta$, corresponds to $m = 1$. More generally, the line segment $\frac{1-\beta}{1-\alpha} = m$ passes through $(\alpha, \beta) = (1, 1)$, whose slope is m .
- The left edge of Δ , where $\alpha + \beta = -\frac{5}{2}$, corresponds to $\frac{18}{1-\alpha} = \ell_2^P$.
- $\frac{18}{1-\alpha}$ can be made as large as desired for α sufficiently close to 1 such that $\alpha < \beta < 1$, that is, in the upper right corner of Δ .

More generally, for any $m \in (0, 1)$ and for any $\ell \in (\ell_2^P, \infty)$, recalling $\ell_2^P = 4 + 4m$, there exists $(\alpha, \beta, \gamma) \in \Delta$ such that

$$\frac{\gamma - \beta}{\gamma - \alpha} = m \quad \text{and} \quad \frac{6(2\gamma + 1)}{\gamma - \alpha} = \ell.$$

We summarize our conclusion.

Corollary 3. *Let $(\alpha, \beta, \gamma) \in \Delta$ and \mathbf{u} denotes a periodic traveling wave of (2.1), c the wave speed and T the period, depending on m and a , whence depending on α, β, γ . If*

$$\frac{1}{a^2} < m - 2 + 2\sqrt{1 - m + 4m^2}$$

or

$$1 - 2m - 2\sqrt{4 - m + m^2} < \frac{1}{a^2} < 1 + m - 2\sqrt{4 - 7m + 4m^2}$$

then the spectrum of (2.13) tends to infinity along $\pm\sigma + i\mathbb{R}$ for some $\sigma > 0$.

The bullet points in the regions g_2 and g_3 of Figure 4, for which (2.23) is in the second and third gaps, correspond to the values of α, β, γ for the left panel of Figure 2 and the right panel of Figure 1, respectively. The spectrum in each of the panels tends towards infinity along $\pm\sigma + i\mathbb{R}$ for some $\sigma > 0$. The bullet points in the regions b_3 and b_∞ , for which (2.23) is in the bands (ℓ_3^P, ℓ_3^A) and (ℓ_4^A, ∞) , on the other hand, correspond to the values of α, β, γ for the right panel of Figure 2 and the left panel of Figure 1. The spectrum tends towards infinity along the imaginary axis.

3 The Benney–Luke equation

We turn our attention to (1.4), where $a = 0$ and, for simplicity of notation, $b = 1$, that is,

$$u_{tt} - u_{xx} - u_{xxtt} + u_t u_{xx} + 2u_x u_{xt} = 0, \quad (3.1)$$

whose dispersion relation

$$\omega^2(k) = \frac{k^2}{1 + k^2}$$

remains bounded for all $k \in \mathbb{R}$. Proceeding as in [1, 23], let

$$v = u_x \quad \text{and} \quad w = (1 - \partial_x^2)u_t + \frac{1}{2}v^2, \quad (3.2)$$

and we rewrite (3.1) as

$$\begin{pmatrix} v \\ w \end{pmatrix}_t = \begin{pmatrix} (1 - \partial_x^2)^{-1}(w - \frac{1}{2}v^2) \\ v - v(1 - \partial_x^2)^{-1}(w - \frac{1}{2}v^2) \end{pmatrix}_x. \quad (3.3)$$

Throughout the section, $\mathbf{v} = \begin{pmatrix} v \\ w \end{pmatrix}$. We remark that (3.3) is in the Hamiltonian form, for which

$$H(\mathbf{v}) = \frac{1}{2} \int \left(v^2 + \left(w - \frac{1}{2}v^2 \right) (1 - \partial_x^2)^{-1} \left(w - \frac{1}{2}v^2 \right) \right) dx$$

is the Hamiltonian. In addition to H , (3.3) has three conserved quantities

$$P(\mathbf{v}) = \int vw \, dx, \quad M_1(\mathbf{v}) = \int v \, dx \quad \text{and} \quad M_2(\mathbf{v}) = \int w \, dx.$$

3.1 Parametrization of periodic traveling waves

Similarly as in Section 2.1, a traveling wave of (3.3) takes the form $\mathbf{v}(x - ct - x_0)$ for some $c \neq 0, \infty \in \mathbb{R}$ for some $x_0 \in \mathbb{R}$, and it satisfies

$$\delta(H + cP + b_1 M_1 + b_2 M_2)(\mathbf{v}) = \mathbf{0}$$

for some $b_1, b_2 \in \mathbb{R}$. That is,

$$\begin{aligned} v - v(1 - \partial_x^2)^{-1} \left(w - \frac{1}{2}v^2 \right) + cw + b_1 &= 0, \\ (1 - \partial_x^2)^{-1} \left(w - \frac{1}{2}v^2 \right) + cv + b_2 &= 0. \end{aligned} \quad (3.4)$$

We restrict our attention to periodic solutions of (3.4). The first equation of (3.2) implies that v has mean zero over one period. Also the second equation of (3.2) implies that $w - \frac{1}{2}v^2 = -c(1 - \partial_x^2)u_x$

has mean zero over the period. Therefore the second equation of (3.4) dictates that $b_2 = 0$. In what follows, we drop the subscript and refer to b_1 as b for simplicity of notation. Eliminating w from (3.4), we arrive at

$$c^2 v'' + \frac{3}{2} c v^2 + (1 - c^2) v + b = 0. \quad (3.5)$$

Multiplying (3.5) through by v' and integrating, moreover,

$$\frac{1}{2} c^2 (v')^2 = E - \frac{1}{2} c v^3 - \frac{1}{2} (1 - c^2) v^2 - b v =: E - V(v; c, b) \quad (3.6)$$

for some $E \in \mathbb{R}$. Since (3.6) remains invariant under

$$v \mapsto -v \quad \text{and} \quad (c, b, E) \mapsto (-c, -b, E),$$

we can take $c > 0$ without loss of generality. Since (3.6) remains invariant under the translation of the x axis, we can mod out x_0 .

One can work out the existence of non-constant periodic solutions of (3.6) and, hence, non-constant periodic traveling waves of (3.3), depending on c, b, E , or depending on the roots of the cubic polynomial $E - V(v; c, b)$. But it is inconvenient to impose that v has mean zero over the period when one parametrizes the solutions by the roots of $E - V(v; c, b)$. Instead we restrict our attention to $c > 0$ and give periodic and mean-zero solutions of (3.5) in closed form in terms of the Jacobi elliptic functions:

$$v(x) = \frac{4ma^2}{\sqrt{1 + 4(1 + m - 3mM(m))a^2}} (\text{sn}^2(ax, \sqrt{m}) - M(m)), \quad (3.7)$$

where

$$M(m) := \frac{K(\sqrt{m}) - E(\sqrt{m})}{mK(\sqrt{m})}. \quad (3.8)$$

Here $m \in (0, 1)$ is the elliptic parameter, and

$$K(\sqrt{m}) = \int_0^1 \frac{ds}{\sqrt{(1-s^2)(1-ms^2)}} \quad \text{and} \quad E(\sqrt{m}) = \int_0^1 \sqrt{\frac{1-ms^2}{1-s^2}} ds$$

are the complete elliptic integrals of the first and second kinds (not to be confused with E in (3.6)). Particularly, (3.7) has mean zero over the period

$$T = \frac{2K(\sqrt{m})}{a}. \quad (3.9)$$

A straightforward calculation reveals that

$$\begin{aligned} c &= \frac{1}{\sqrt{1 + 4(1 + m - 3mM(m))a^2}} (> 0), \\ b &= \frac{8(1 - 2(1 + m)M(m) + 3mM^2(m))ma^4}{\sqrt{1 + 4(1 + m - 3mM(m))a^2}^3}, \\ E &= \frac{32(1 - M(m))(1 - mM(m))m^2M(m)a^6}{(1 + 4(1 + m - 3mM(m))a^2)^2}. \end{aligned} \quad (3.10)$$

We take $a > 0$ without loss of generality. If $m \leq m_0$, where

$$m_0 \approx 0.961 \text{ is the unique root of } 1 + m - 3mM(m), \quad (3.11)$$

then (3.7) is defined for all a . If $m > m_0$, on the other hand, then $a < \frac{1}{2\sqrt{3mM(m)-m-1}}$ must hold true.

To summarize, whenever

$$(m, a) \in \square := \left\{ (m, a) \in (0, 1) \times (0, \infty) : a < \frac{1}{2\sqrt{3mM(m)-m-1}} \text{ for } m < m_0 \right\}, \quad (3.12)$$

where m_0 is in (3.11), (3.7) and (3.8) give a periodic traveling wave of (3.3), depending on m and a , and v has mean zero over the period. Figure 5 shows \square in the (m, a) plane.

3.2 Asymptotic spectral analysis to short wavelength perturbations

Let $(m, a) \in \square$ (see (3.12)) and \mathbf{v} denotes a periodic traveling wave of (3.3) (see (3.4), (3.7), (3.8)), c the wave speed (see (3.10)) and T the period (see (3.9)), depending on m and a . Linearizing (3.3) about \mathbf{v} in the moving frame of reference, and seeking a solution of the form $e^{\lambda t} \phi(x)$, say, where $\lambda \in \mathbb{C}$, we arrive at

$$\lambda \phi = \begin{pmatrix} \partial_x(c - (1 - \partial_x^2)^{-1}v) & \partial_x(1 - \partial_x^2)^{-1} \\ \partial_x(1 + cv + v(1 - \partial_x^2)^{-1}v) & \partial_x(c - (1 - \partial_x^2)^{-1}v) \end{pmatrix} \phi =: \mathbf{L}(\mathbf{v})\phi. \quad (3.13)$$

Similarly as in Section 2.2, \mathbf{v} is spectrally stable if and only if the spectrum of $\mathbf{L}(\mathbf{v}) : H^1(\mathbb{R}) \times H^1(\mathbb{R}) \subset L^2(\mathbb{R}) \times L^2(\mathbb{R}) \rightarrow L^2(\mathbb{R}) \times L^2(\mathbb{R})$ is contained in the imaginary axis. Similarly as in Section 2.2, λ is in the spectrum of $\mathbf{L}(\mathbf{v})$ if and only if (3.13) has a nontrivial bounded solution such that

$$\phi(x + T) = e^{\frac{2\pi i k x}{T}} \phi(x) \quad \text{for some } k \in \mathbb{R}.$$

We focus our attention to $|k| \gg 1$.

Similarly as in Section 2.2, let

$$\lambda = \lambda^{(1)}k + \lambda^{(0)} + \lambda^{(-1)}k^{-1} + \dots \quad \text{and} \quad \phi(x) = e^{\frac{2\pi i k x}{T}} (\phi^{(0)}(x) + \phi^{(-1)}(x)k^{-1} + \phi^{(-2)}(x)k^{-2} + \dots)$$

as $|k| \rightarrow \infty$ for some $\lambda^{(1)}, \lambda^{(0)}, \lambda^{(-1)}, \dots \in \mathbb{C}$ for some $\phi^{(0)}, \phi^{(-1)}, \phi^{(-2)}, \dots \in L^\infty(\mathbb{R}) \times L^\infty(\mathbb{R})$, so that (3.13) becomes

$$\begin{aligned} & (\lambda^{(1)}k + \lambda^{(0)} + \lambda^{(-1)}k^{-1} + \dots)(\phi^{(0)} + \phi^{(-1)}k^{-1} + \phi^{(-2)}k^{-2} + \dots) \\ &= \begin{pmatrix} \left(\frac{2\pi i k}{T} + \partial_x\right)(c - (1 - (\frac{2\pi i k}{T} + \partial_x)^2)^{-1}v) & (\frac{2\pi i k}{T} + \partial_x)(1 - (\frac{2\pi i k}{T} + \partial_x)^2)^{-1} \\ \left(\frac{2\pi i k}{T} + \partial_x\right)(1 + cv + v(1 - (\frac{2\pi i k}{T} + \partial_x)^2)^{-1}v) & (\frac{2\pi i k}{T} + \partial_x)(c - (1 - (\frac{2\pi i k}{T} + \partial_x)^2)^{-1}v) \end{pmatrix} \\ & \quad \cdot (\phi^{(0)} + \phi^{(-1)}k^{-1} + \phi^{(-2)}k^{-2} + \dots) \end{aligned}$$

as $|k| \rightarrow \infty$, where

$$\left(1 - \left(\frac{2\pi i k}{T} + \partial_x\right)^2\right)^{-1} = \frac{T^2}{4\pi^2 k^2} + O(k^{-3}) \quad \text{as } |k| \rightarrow \infty.$$

At the order of k , we gather

$$\lambda^{(1)}\phi^{(0)} = \begin{pmatrix} \frac{2\pi i c}{T} & 0 \\ \frac{2\pi i}{T}(1 + cv) & \frac{2\pi i c}{T} \end{pmatrix} \phi^{(0)},$$

whence

$$\lambda^{(1)} = \frac{2\pi ic}{T} \quad \text{and} \quad \phi^{(0)} = \begin{pmatrix} 0 \\ \phi_2^{(0)} \end{pmatrix},$$

where $\phi_2^{(0)}$ is bounded and otherwise arbitrary. At the order of 1, we gather

$$\lambda^{(1)}\phi^{(-1)} + \lambda^{(0)}\phi^{(0)} = \begin{pmatrix} \frac{2\pi ic}{T} & 0 \\ \frac{2\pi i}{T}(1+cv) & \frac{2\pi ic}{T} \end{pmatrix}\phi^{(-1)} + \begin{pmatrix} c\partial_x & 0 \\ \partial_x(1+cv) & c\partial_x \end{pmatrix}\phi^{(0)}$$

or, equivalently,

$$\begin{pmatrix} 0 & 0 \\ \frac{2\pi i}{T}(1+cv) & 0 \end{pmatrix}\phi^{(-1)} = \begin{pmatrix} 0 \\ (\lambda^{(0)} - c\partial_x)\phi_2^{(0)} \end{pmatrix},$$

whence

$$\frac{2\pi i}{T}(1+cv)\phi_1^{(-1)} = (\lambda^{(0)} - c\partial_x)\phi_2^{(0)}.$$

At the order of k^{-1} , similarly,

$$\begin{aligned} \lambda^{(1)}\phi^{(-2)} + \lambda^{(0)}\phi^{(-1)} + \lambda^{(-1)}\phi^{(0)} \\ = \begin{pmatrix} \frac{2\pi ic}{T} & 0 \\ \frac{2\pi i}{T}(1+cv) & \frac{2\pi ic}{T} \end{pmatrix}\phi^{(-2)} + \begin{pmatrix} c\partial_x & 0 \\ \partial_x(1+cv) & c\partial_x \end{pmatrix}\phi^{(-1)} + \begin{pmatrix} -\frac{T}{2\pi i}v & \frac{T}{2\pi i} \\ \frac{T}{2\pi i}v^2 & -\frac{T}{2\pi i}v \end{pmatrix}\phi^{(0)} \end{aligned}$$

or, equivalently,

$$\begin{pmatrix} 0 & 0 \\ \frac{2\pi i}{T}(1+cv) & 0 \end{pmatrix}\phi^{(-2)} = \begin{pmatrix} (\lambda^{(0)} - c\partial_x)\phi_1^{(-1)} - \frac{T}{2\pi i}\phi_2^{(0)} \\ -\partial_x((1+cv)\phi_1^{(-1)}) + (\lambda^{(0)} - c\partial_x)\phi_2^{(-1)} + (\lambda^{(-1)} + \frac{T}{2\pi i}v)\phi_2^{(0)} \end{pmatrix},$$

which is solvable by the Fredholm alternative, provided that

$$(\lambda^{(0)} - c\partial_x)\phi_1^{(-1)} - \frac{T}{2\pi i}\phi_2^{(0)} = 0.$$

Therefore

$$((\lambda^{(0)} - c\partial_x)^2 - (1+cv))\phi_1^{(-1)} = 0. \quad (3.14)$$

Similarly as in Section 2.2, if the Hill's differential equation

$$c^2y'' - (1+cv)y = 0 \quad (3.15)$$

is elliptic (in a band), so that (3.14) has a bounded solution if and only if $\text{Re}(\lambda^{(0)}) = 0$, then the spectrum of (3.13) tends to infinity along the imaginary axis. If (3.15) is hyperbolic (in a gap), on the other hand, so that (3.14) has a bounded solution if and only if $\text{Re}(\lambda^{(0)}) = \pm\sigma$, where $\sigma > 0$ is the Lyapunov exponent of (3.15), then the spectrum tends to infinity along $\pm\sigma + i\mathbb{R}$.

Similarly as in Section 2.4, after the change of variables $x \mapsto \frac{x}{a}$, we can rewrite (3.15) as the Lamé equation

$$y'' - 4m \text{sn}^2(x, \sqrt{m})y = \ell y, \quad (3.16a)$$

where

$$\ell = \frac{1}{a^2} + 4(1+m-4mM(m)) \quad (3.16b)$$

by (3.7) and (3.10). Let $\{\ell_j^P\}_{j=1}^\infty$ denote the periodic eigenvalues of (3.16a) and $\{\ell_j^A\}_{j=1}^\infty$ the anti-periodic eigenvalues such that

$$-\infty < \ell_1^P < \ell_1^A \leq \ell_2^A < \ell_2^P \leq \ell_3^P < \ell_3^A \leq \ell_4^A < \dots .$$

If (3.16) lies in a band, that is, (3.16b) is in

$$(\ell_1^P, \ell_1^A) \cup (\ell_2^A, \ell_2^P) \cup (\ell_3^P, \ell_3^A) \cup \dots ,$$

then the spectrum of (3.13) tends to infinity along the imaginary axis. If (3.16) is in a gap, that is,

$$(-\infty, \ell_1^P) \cup (\ell_1^A, \ell_2^A) \cup (\ell_2^P, \ell_3^P) \cup \dots ,$$

on the other hand, then the spectrum tends to infinity along $\pm\sigma + i\mathbb{R}$ for some $\sigma > 0$. We refer to $(-\infty, \ell_1^P)$ as the zeroth gap for convenience.

But one difference with Section 2.4 is that (3.16a) is not a finite-gap Lamé equation, whereby analytical formulae of the eigenvalues seem not viable to use. Nevertheless we can compute the band edges numerically. Of practical usefulness to this end is [19]

$$\operatorname{sn}^2(x, \sqrt{m}) = M(m) - \frac{2\pi^2}{mK^2(\sqrt{m})} \sum_{k=1}^{\infty} \frac{kq^k}{1-q^{2k}} \cos\left(\frac{\pi kx}{K(\sqrt{m})}\right),$$

where

$$q = e^{-\frac{\pi K'(\sqrt{m})}{K(\sqrt{m})}}, \quad K'(\sqrt{m}) = K(\sqrt{m'}) \quad \text{and} \quad m' = 1 - m.$$

Suppose that

$$y(x) = \sum_{k \in \mathbb{Z}} \hat{y}_k e^{\frac{\pi i k x}{K}}, \quad \hat{y}_k \text{ are the Fourier coefficients,}$$

and we consider (3.16) in the basis $\{e^{\frac{\pi i k x}{K}} : k \in \mathbb{Z}\}$ of $L^2(-K, K)$ subject to the periodic boundary condition. We make the Fourier collocation projection of (3.16) to the subspace spanned by $\{e^{\frac{\pi i k x}{K}} : k \in (-N_k, N_k)\}$ (here $N_k = 50$) and solve numerically the resulting eigenvalue problem for a diagonal matrix plus a Toeplitz matrix, approximating numerically the periodic eigenvalues. We take the basis $\{e^{\frac{\pi i k x}{K} + \frac{\pi i x}{2K}} : k \in \mathbb{Z}\}$ of $L^2(-K, K)$ subject to $y(K) = -y(-K)$ for the anti-periodic eigenvalues.

Figure 5 shows bands and gaps of (3.16) in the (m, a) plane. Similarly to Section 2.4, not all bands and gaps are present in \square . Specifically, the zeroth gap and the first band are not present. We expect that (3.16a) has countably many gaps and all are open. There is no proof, however, to the best of the authors' knowledge. Figure 5 shows the j -th gaps, $j = 1, 2, 3$, and the j -th bands, $j = 2, 3, 4$. The j -th gaps, $j \geq 4, \in \mathbb{Z}$, in the region labelled 'higher bands and gaps', are exceedingly narrow in the (m, a) plane, for which the spectrum of (3.13) would tend to infinity along $\pm\sigma + i\mathbb{R}$ for σ exceedingly small. Such instability would not be of profound physical significance.

We summarize our conclusion.

Theorem 4. *Let $(m, a) \in \square$ and \mathbf{v} denotes a periodic traveling wave of (3.3), c the wave speed and T the period, depending on m and a . Let $\{\ell_j^P\}_{j=1}^\infty$ denote the periodic eigenvalues of (3.16a) and $\{\ell_j^A\}_{j=1}^\infty$ the anti-periodic eigenvalues. If*

$$\frac{1}{\sqrt{\ell_{2j}^A - 4(1+m-4mM(m))}} < a < \frac{1}{\sqrt{\ell_{2j-1}^A - 4(1+m-4mM(m))}} \quad \text{for } j \geq 2, \in \mathbb{Z},$$

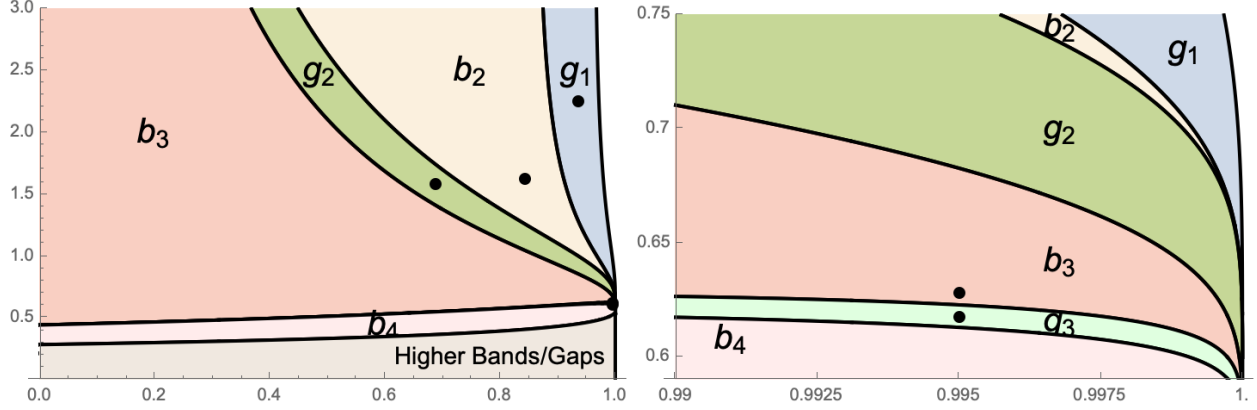


Figure 5: \square in the (m, a) plane: $g_j, j \geq 1, \in \mathbb{Z}$, denotes the region, for which (3.16) is in the j -th gap, that is, (3.16b) is in (ℓ_j^P, ℓ_{j+1}^P) for j even and (ℓ_j^A, ℓ_{j+1}^A) for j odd. Also $b_j, j \geq 2, \in \mathbb{Z}$, denotes the j -th band, that is, (ℓ_j^A, ℓ_j^P) for j even and (ℓ_j^P, ℓ_j^A) for j odd. The j -th gaps, $j \geq 4, \in \mathbb{Z}$, and the j -th bands, $j \geq 5, \in \mathbb{Z}$, are in the region labelled ‘higher bands and gaps’. The bullet points correspond to the values of (m, a) for Figures 6-10. On the right is a close-up for the values of (m, a) for Figures 9 and 10.

or

$$\frac{1}{\sqrt{\ell_{2j+1}^P - 4(1+m-4mM(m))}} < a < \frac{1}{\sqrt{\ell_{2j}^P - 4(1+m-4mM(m))}} \quad \text{for } j \geq 1, \in \mathbb{Z},$$

so that (3.16) is in a gap, then the spectrum of (3.13) tends to infinity along $\pm\sigma + i\mathbb{R}$ for some $\sigma > 0$.

3.3 Numerical experiments

Similarly as in Section 2.3, we compute the spectrum of (3.13) numerically by a Fourier spectral method. One minor difference is that we integrate (3.5) numerically and approximate the Fourier coefficients by numerical quadrature, without recourse to an analytic formula for the Jacobi elliptic function. Similarly as in Section 2.3, when (3.15) is in a gap, we integrate (3.15) numerically and approximate numerically the eigenvalues of the monodromy matrix.

Figures 6, 8, 10 provide examples of the numerically computed spectrum of (3.13), for which (3.16) lies in the j -th gap, $j = 1, 2, 3$, respectively. The values of m and a correspond to the bullet points in the regions g_j of Figure 5, $j = 1, 2, 3$. The numerical result corroborates Theorem 4 that the spectrum tends towards infinity along $\pm\sigma + i\mathbb{R}$ for some $\sigma > 0$. In each of the examples, σ agrees well with $\frac{\log(|\mu|)}{T}$, where μ is the numerically computed eigenvalue of the monodromy matrix of (3.15) such that $|\mu| > 1$. Notice modulational instability to long wavelength perturbations near $0 \in \mathbb{C}$ in each example, and spectral instability to finite wavelength perturbations away from $0 \in \mathbb{C}$ in Figure 10.

Figures 7 and 9 show examples of the spectrum, for which (3.16) is in the j -th band, $j = 2$ and 3, respectively. Recall that there are no values of m and a for which (3.16) is in the first band. The numerical result supports our analytical prediction that the spectrum tends towards infinity along the imaginary axis. Notice modulational instability in each of the examples and finite wavelength instability in Figure 9.

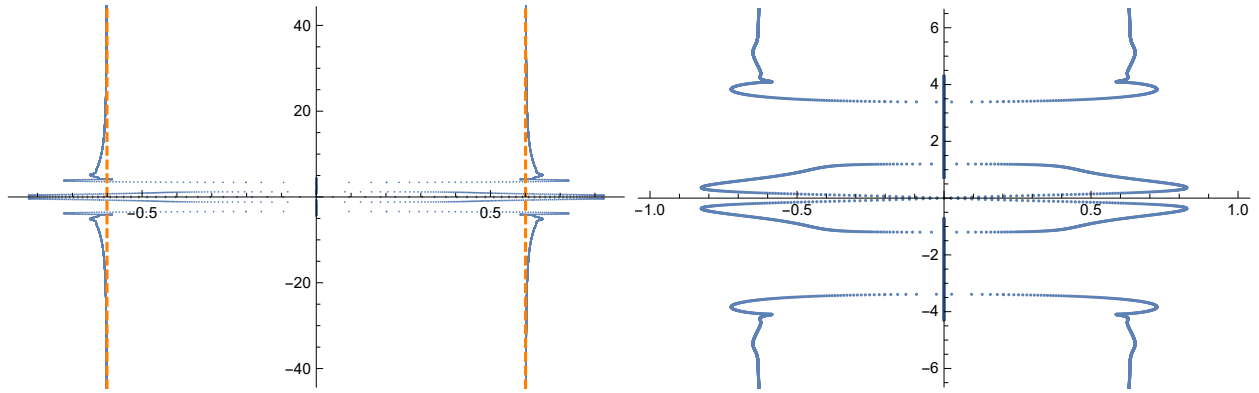


Figure 6: The numerically computed spectrum of (3.13), where v, c, T depend on $m = 0.9342$ and $a = 2.25$, for which (3.16) is in the first gap. The spectrum tends towards infinity along the dashed lines $\pm\sigma + i\mathbb{R}$, where $\sigma \approx 0.600755$. On the right is a close-up for modulational instability near $0 \in \mathbb{C}$.

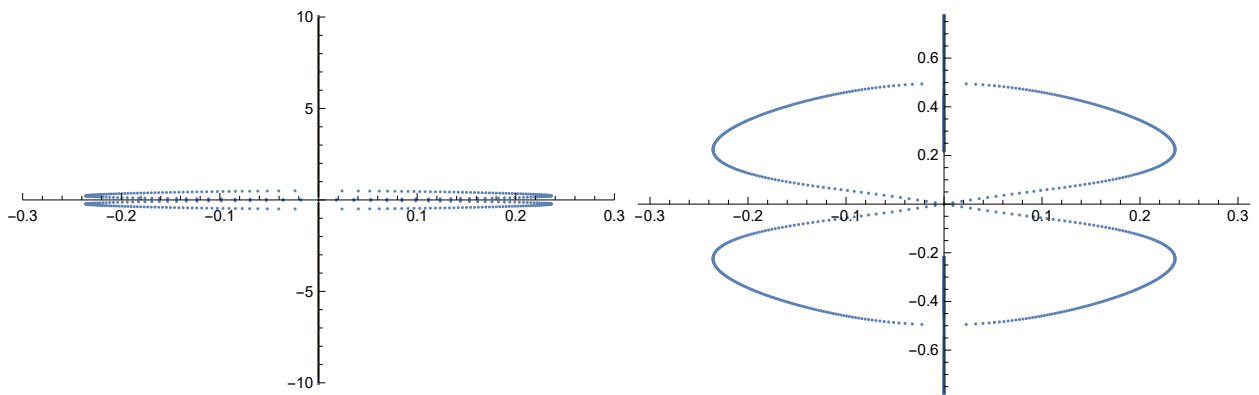


Figure 7: The spectrum of (3.13) for $m = 0.8428$ and $a = 1.621$, for which (3.16) is in the second band. The spectrum lies along the imaginary axis far away from $0 \in \mathbb{C}$. On the right is a close-up for modulational instability.

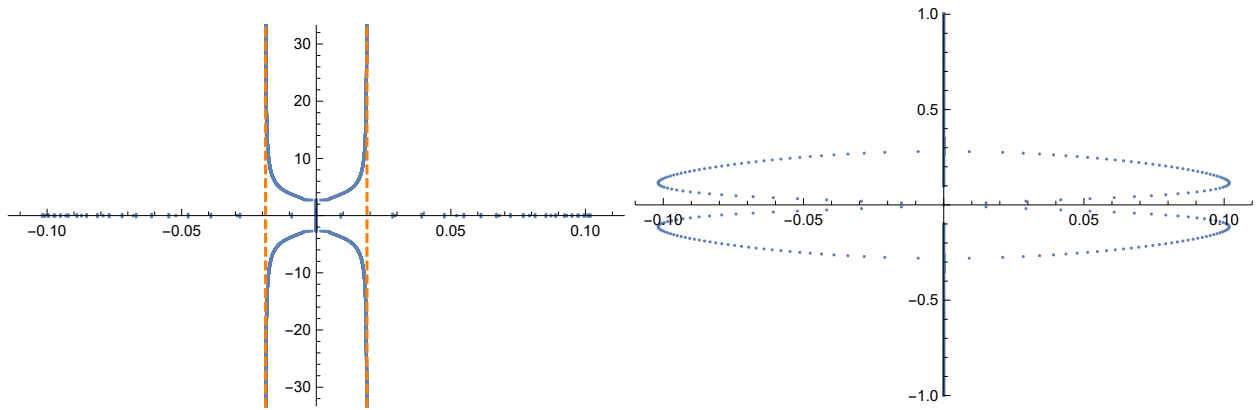


Figure 8: The spectrum of (3.13) for $m = 0.6872$ and $a = 1.584$, for which (3.16) is in the second gap. The spectrum tends towards infinity along the dashed lines $\pm\sigma + i\mathbb{R}$, where $\sigma \approx 0.0188322$. On the right is a close up for modulational instability near $0 \in \mathbb{C}$.

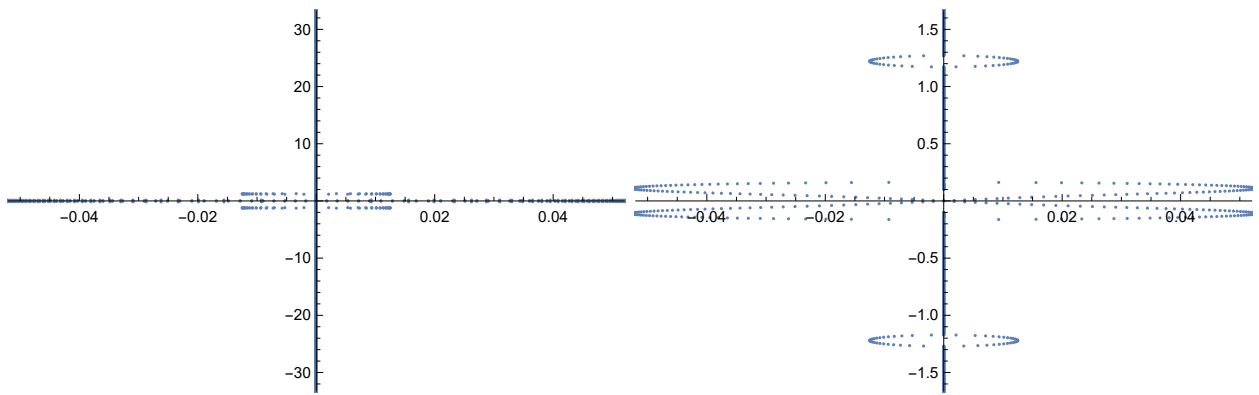


Figure 9: The spectrum of (3.13) for $m = 0.995$ and $a = 0.628$, for which (3.16) is in the third band. The spectrum lies along the imaginary axis far away from $0 \in \mathbb{C}$. On the right is a close up for modulational instability near $0 \in \mathbb{C}$ and finite wavelength instability near $\pm 1.25i$.

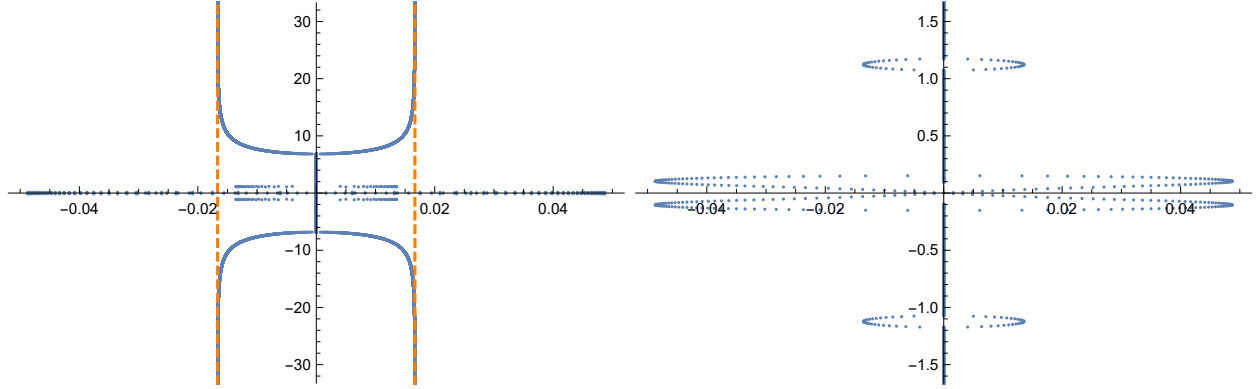


Figure 10: The spectrum of (3.13) for $m = 0.995$ and $a = 0.618$, for which (3.16) is in the third gap. The spectrum tends towards infinity along the dashed lines $\pm\sigma + i\mathbb{R}$, where $\sigma \approx 0.016658$. On the right is a close-up for modulational instability near $0 \in \mathbb{C}$ and finite wavelength instability near $\pm 1.1i$.

4 The coupled Benjamin–Bona–Mahony system

Last but not least, we turn to (1.5), where $a = c = 0$ and $b = d = \frac{1}{6}$, that is,

$$\begin{aligned} \eta_t + u_x - \frac{1}{6}\eta_{xxt} + (\eta u)_x &= 0, \\ u_t + \eta_x - \frac{1}{6}u_{xxt} + uu_x &= 0, \end{aligned} \tag{4.1}$$

whose dispersion relation

$$\omega^2(k) = \frac{k^2}{(1 + \frac{1}{6}k^2)(1 + \frac{1}{6}k^2)}$$

remains bounded for all $k \in \mathbb{R}$. We remark that $b = d = \frac{1}{6}$ is for convenience and better correspondence to earlier works [5, 6].

4.1 Parametrization of periodic traveling waves

A traveling wave of (4.1) takes the form $\eta(x - ct - x_0)$ and $u(x - ct - x_0)$ for some $c \neq 0, \in \mathbb{R}$ for some $x_0 \in \mathbb{R}$, and they satisfy by quadrature

$$\begin{aligned} -c\eta + u + \frac{1}{6}c\eta'' + u\eta &= b_1, \\ -cu + \eta + \frac{1}{6}cu'' + \frac{1}{2}u^2 &= b_2 \end{aligned} \tag{4.2}$$

for some $b_1, b_2 \in \mathbb{R}$. Periodic solutions of (4.2) were treated in [13, 12], among others, but for $b_1 = b_2 = 0$, and not exhaustively, to the best of the authors' knowledge. Here we work out all $b_1, b_2 \in \mathbb{R}$. Similarly as in Sections 2.1 and 3.1, we can mod out x_0 .

Eliminating η from (4.2), we arrive at

$$c^2u'''' + (u - c)(12cu'' + 18u^2 - 36cu + b_2) + 6c(u')^2 - 36u + b_1 = 0. \tag{4.3}$$

Suppose that a solution of (4.3) satisfies

$$u'' = P(u; c, b_1, b_2), \quad P \text{ is a polynomial of } u,$$

allowing for elliptic and hyperelliptic functions, whence

$$\frac{1}{2}(u')^2 = Q(u; c, b_1, b_2), \quad Q' = P, \quad (4.4a)$$

and also

$$u'''' = 2(P''Q + PP')(u; c, b_1, b_2).$$

Substituting into (4.3), we deduce that $\deg(Q) \leq 3$, so that no hyperelliptic functions. Assuming that $\deg(Q) = 3$, after some algebra we find

$$Q(u; c, b_1, b_2) = -\frac{3}{5c}u^3 + \frac{9}{5}u^2 - \frac{144c^2 + 25b_2 - 900}{330c}u - \frac{1008c^3 - 6300c + 275b_1 - 100b_2c}{1320c}. \quad (4.4b)$$

One can work out the existence of non-constant periodic solutions of (4.4) and, hence, non-constant periodic traveling waves of (4.1), provided that the discriminant

$$\begin{aligned} \text{disc}(Q) := & \frac{1}{76665c^4} (4665600c^6 + 27993600c^4 - 363181968c^2 \\ & - 777600b_2c^4 + 43200b_2^2c^2 - 3110400b_2c^2 + 23287176b_1c \\ & - 323433b_1^2 - 800b_2^3 + 86400b_2^2 - 3110400b_2 + 37324800) \end{aligned} \quad (4.5)$$

is positive. When $b_1 = b_2 = 0$, (4.5) has simple roots at $c = \pm\frac{5}{2}$ and $\pm\frac{1}{2}\sqrt{\frac{33\sqrt{57}}{10} - \frac{49}{2}} \approx \pm 0.3219$, together with a pole at zero, so that (4.4) has periodic solutions, provided that

$$c \in \left(-\infty, -\frac{5}{2}\right) \cup \left(-\frac{1}{2}\sqrt{\frac{33\sqrt{57}}{10} - \frac{49}{2}}, 0\right) \cup \left(0, \frac{1}{2}\sqrt{\frac{33\sqrt{57}}{10} - \frac{49}{2}}\right) \cup \left(\frac{5}{2}, \infty\right).$$

This reproduces the result of [12].

More generally, (4.4) has periodic solutions, provided that c is in some interval, depending on b_1 and b_2 , for which (4.5) is positive. The number of intervals of such ‘admissible’ wave speeds is constant in open sets in the (b_1, b_2) plane and changes across the curves of co-dimension one, which can be found in closed form:

$$\begin{aligned} b_1^2 &= \frac{800}{323433}(36 - b_2)^3, \\ b_1^2 &= \frac{16}{1617165} \left(-125b_2^3 + 13500b_2^2 + 4365495b_2 - 168821820 + \sqrt{25b_2^2 - 1800b_2 + 35583}^3 \right), \quad (4.6) \\ b_1^2 &= 72b_2 - 2592. \end{aligned}$$

Figure 11 shows the regions in the (b_1, b_2) plane, in each of which the number of intervals of admissible wave speeds is constant, denoted by the label, and whose boundaries are made up of the curves in (4.6). For any $b_1, b_2 \in \mathbb{R}$, (4.5) is positive when $|c|$ becomes sufficiently large, so that (4.4) has a periodic solution, whereas no solutions when $c = 0$. Therefore the number of intervals of admissible wave speeds is ≥ 2 .

For (b_1, b_2) in the region 4 of Figure 11, there are four intervals of admissible wave speeds, two where $c > 0$ and two where $c < 0$. They are symmetric about $c = 0$ when $b_1 = 0$ and asymmetric

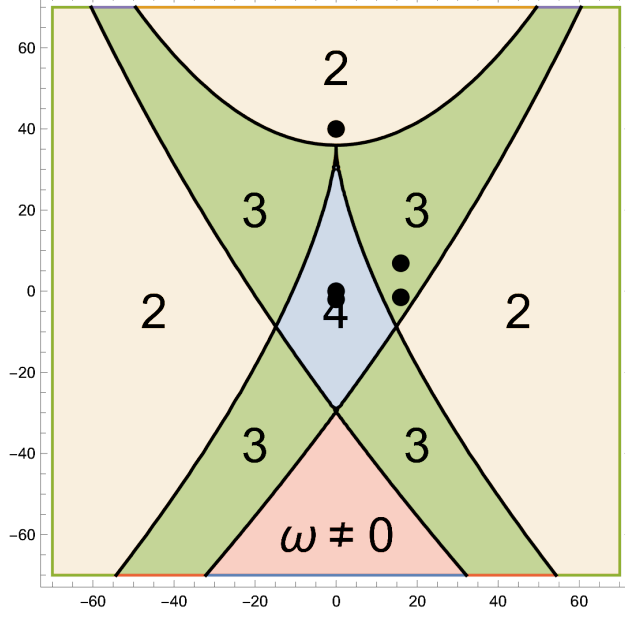


Figure 11: Regions in the (b_1, b_2) plane, separated by the curves in (4.6), in each of which the number of intervals of admissible wave speeds is constant and denoted by the label. In the region $c \neq 0$, the intervals of admissible wave speeds are $(-\infty, 0)$ and $(0, \infty)$. The bullet points correspond to the values of b_1 and b_2 for Figures 12–17.

otherwise. Particularly, $(b_1, b_2) = (0, 0)$ is in the region 4, which was treated in [12, 13] and others. For (b_1, b_2) in the region 3, the number of intervals of admissible wave speeds is three, and in the remaining regions, it is two. In the region $c \neq 0$, where b_1 and b_2 satisfy

$$b_1^2 < \frac{16}{1617165} \left(-125b_2^3 + 13500b_2^2 + 4365495b_2 - 168821820 + \sqrt{25b_2^2 - 1800b_2 + 355833}^3 \right)$$

and $b_2 < \frac{9}{5}(20 - 11\sqrt{11})$, the number of intervals of admissible wave speeds is two, but we single it out because the intervals are $(-\infty, 0)$ and $(0, \infty)$. In other words, the only inadmissible wave speed is zero. In all the other regions, by contrast, there is a (nonempty) closed interval of inadmissible wave speeds.

Actually, periodic solutions of (4.4) can be found in closed form in terms of the Jacobi elliptic functions. Recall that $y(x) = \frac{2m-1}{3} - m \operatorname{cn}^2(x, \sqrt{m})$ is a solution of

$$(y')^2 = 4y^3 - \frac{4}{3}(1 - m + m^2)y - \frac{4}{27}(2 - 3m - 3m^2 + 2m^3),$$

where $m \in (0, 1)$ is an elliptic operator. After appropriate changes of variables, notice that

$$z(x) = z_0 \left(\frac{2m-1}{3} - m \operatorname{cn}^2(ax, \sqrt{m}) \right)$$

is a solution of

$$(z')^2 = \alpha_3 z^3 + \alpha_1 z + \alpha_0,$$

where

$$z_0 = \frac{9\alpha_0(1 - m + m^2)}{\alpha_1(2 - 3m - 3m^2 + 2m^3)} \quad \text{and} \quad a = \sqrt{\frac{9\alpha_0\alpha_3(1 - m + m^2)}{4\alpha_1(2 - 3m - 3m^2 + 2m^3)}}, \quad (4.7)$$

if and only if

$$-\frac{(2-3m-3m^2+2m^3)^2}{27(1-m+m^2)^3} = \frac{\alpha_0^2 \alpha_3}{\alpha_1^3} \in \left(-\frac{4}{27}, 0\right) \quad (4.8)$$

for some $m \in (0, 1)$. The left hand side of (4.8) increases monotonically from $-\frac{4}{27}$ at $m = 0$ to 0 at $m = \frac{1}{2}$, and then decreases monotonically to $-\frac{4}{27}$ at $m = 1$. Therefore whenever $\frac{\alpha_0^2 \alpha_3}{\alpha_1^3} \in \left(-\frac{4}{27}, 0\right)$, (4.8) has exactly two solutions in the interval $(0, 1)$, one less than $\frac{1}{2}$ and one greater than $\frac{1}{2}$. But a (see (4.7)) is real only for one of the solutions. If $\alpha_0 > 0$ then we must choose the solution of (4.8) in the interval $(0, \frac{1}{2})$, and if $\alpha_0 < 0$ then $(\frac{1}{2}, 1)$.

Returning to (4.4), let $u = v + c$, and after some algebra we arrive at

$$(v')^2 = -\frac{6}{5c}v^3 + \frac{90c^2 - 5b_2 + 180}{66c}v + \frac{-5b_1 + 180}{24c} =: \alpha_3 v^3 + \alpha_1 v + \alpha_0,$$

so that whenever (4.8) holds true for some $m \in (0, 1)$, depending on c, b_1, b_2 ,

$$u(x) = c + u_0 \left(\frac{2m-1}{3} - m \operatorname{cn}^2(ax, \sqrt{m}) \right)$$

gives a periodic solution of (4.4), where $u_0 = \frac{9\alpha_0(1-m+m^2)}{\alpha_1(2-3m-3m^2+2m^3)}$ and a is in (4.7), whose period is $T = \frac{2K(\sqrt{m})}{a}$, where $K(\sqrt{m})$ is the complete elliptic integral of the first kind.

Remark. Periodic solutions of (4.4) can also be found in terms of the Weierstrass elliptic functions as

$$u(x) = c - \frac{10}{3}c\wp \left(x; \frac{18c^2 - b_2 + 36}{22c^2}, \frac{-108c + 3b_1}{80c^3} \right),$$

depending on c, b_1, b_2 , where $\wp(x; g_2, g_3)$ denotes the Weierstrass \wp -function, and g_2 and g_3 are the elliptic invariants. When $b_1 = b_2 = 0$, this reproduces the result of [13]. But the account of [13], while mathematically correct, could be misleading. The solution of [13] is given as

$$u(x; c, \Lambda, \delta) = c - \frac{10}{3}\Lambda^2\delta^2c\wp \left(\delta\Lambda x; \frac{9(c^2+2)}{11\Lambda^4\delta^4c^2}, -\frac{27}{20\Lambda^6\delta^6c^2} \right)$$

(after correcting a very minor typo in [13, (B.7)]), where δ is described as free. But the Weierstrass \wp -function enjoys the scaling invariance

$$\lambda^2\wp \left(\lambda x; \frac{g_2}{\lambda^4}, \frac{g_3}{\lambda^6} \right) = \wp(x; g_2, g_3)$$

for any $\lambda \neq 0, \in \mathbb{R}$ (see [25, pp. 439] or [22, (1.41)], for instance). Therefore, the solutions of [13] are independent of Λ and δ , and depend only on c (plus x_0 , but one can mod out x_0).

4.2 Asymptotic spectral analysis to short wavelength perturbations

Let η and u denote a periodic traveling wave of (4.1), c the wave speed, and T the period, whose existence has been established in the previous subsection. Linearizing (4.1) about η and u in the frame of reference moving at the speed c , and seeking a solution of the form $e^{\lambda t}\phi(x)$, say, where $\lambda \in \mathbb{C}$, we arrive at

$$\lambda\phi = \begin{pmatrix} c\partial_x + \partial_x \left(\frac{1}{6}\partial_x^2 - 1 \right)^{-1} u & \partial_x \left(\frac{1}{6}\partial_x^2 - 1 \right)^{-1} (1 + \eta) \\ \partial_x \left(\frac{1}{6}\partial_x^2 - 1 \right)^{-1} & c\partial_x + \partial_x \left(\frac{1}{6}\partial_x^2 - 1 \right)^{-1} u \end{pmatrix} \phi. \quad (4.9)$$

Similarly as in Sections 2.2 and 3.2, η and u are spectrally stable if and only if the spectrum of (4.9) is contained in the imaginary axis, and λ is in the spectrum if and only if (4.9) has a nontrivial bounded solution such that $\phi(x+T) = e^{\frac{2\pi i k x}{T}} \phi(x)$ for some $k \in \mathbb{R}$.

Similarly as in Sections 2.2 and 3.2, let

$\lambda = \lambda^{(1)}k + \lambda^{(0)} + \lambda^{(-1)}k^{-1} + \dots$ and $\phi(x) = e^{\frac{2\pi i k x}{T}}(\phi^{(0)}(x) + \phi^{(-1)}(x)k^{-1} + \phi^{(-2)}(x)k^{-2} + \dots)$ as $|k| \rightarrow \infty$ for some $\lambda^{(1)}, \lambda^{(0)}, \lambda^{(-1)}, \dots \in \mathbb{C}$ for some $\phi^{(0)}, \phi^{(-1)}, \phi^{(-2)}, \dots \in L^\infty(\mathbb{R}) \times L^\infty(\mathbb{R})$, so that (4.9) becomes

$$\begin{aligned} & (\lambda^{(1)}k + \lambda^{(0)} + \lambda^{(-1)}k^{-1} + \dots)(\phi^{(0)} + \phi^{(-1)}k^{-1} + \phi^{(-2)}k^{-2} + \dots) \\ & =: (\mathbf{L}^{(1)}k + \mathbf{L}^{(0)} + \mathbf{L}^{(-1)}k^{-1} + \dots)(\phi^{(0)} + \phi^{(-1)}k^{-1} + \phi^{(-2)}k^{-2} + \dots) \end{aligned}$$

as $|k| \rightarrow \infty$, where

$$\mathbf{L}^{(1)} = \begin{pmatrix} \frac{2\pi i c}{T} & 0 \\ 0 & \frac{2\pi i c}{T} \end{pmatrix}, \quad \mathbf{L}^{(0)} = \begin{pmatrix} c\partial_x & 0 \\ 0 & c\partial_x \end{pmatrix} \quad \text{and} \quad \mathbf{L}^{(-1)} = \begin{pmatrix} -\frac{3Ti}{\pi} & -\frac{3Ti}{\pi}(1+\eta) \\ -\frac{3Ti}{\pi} & -\frac{3Ti}{\pi}u \end{pmatrix}.$$

At the order of k , we gather

$$\lambda^{(1)}\phi^{(0)} = \mathbf{L}^{(1)}\phi^{(0)} = \begin{pmatrix} \frac{2\pi i c}{T} & 0 \\ 0 & \frac{2\pi i c}{T} \end{pmatrix}\phi^{(0)},$$

whence

$$\lambda^{(1)} = \frac{2\pi i c}{T} \quad \text{and} \quad \phi^{(0)} \text{ is bounded and otherwise arbitrary.}$$

At the order of 1,

$$\lambda^{(1)}\phi^{(-1)} + \lambda^{(0)}\phi^{(0)} = \mathbf{L}^{(1)}\phi^{(-1)} + \mathbf{L}^{(0)}\phi^{(0)}.$$

Since $\mathbf{L}^{(1)} - \lambda^{(1)}\mathbf{1} = \mathbf{0}$, where $\mathbf{1}$ denotes the identity operator,

$$\lambda^{(0)}\phi^{(0)} = \mathbf{L}^{(0)}\phi^{(0)} = \begin{pmatrix} c\partial_x & 0 \\ 0 & c\partial_x \end{pmatrix}\phi^{(0)},$$

whence $\phi^{(0)}(x) = e^{c^{-1}\lambda^{(0)}x}\phi$ for some constant ϕ . Seeking a bounded solution, we deduce that $\lambda^{(0)}$ is purely imaginary. On the other hand, $\lambda \sim \lambda^{(1)}k = \frac{2\pi i c k}{T}$ as $|k| \rightarrow \infty$ to leading order, and $\lambda^{(0)}$ amounts to translate such—otherwise arbitrary—spectrum along the imaginary axis. Therefore, without loss of generality,

$$\lambda^{(0)} = 0 \quad \text{and} \quad \phi^{(0)} \text{ is a constant.}$$

At the order of k^{-1} , similarly,

$$\lambda^{(1)}\phi^{(-2)} + \lambda^{(0)}\phi^{(-1)} + \lambda^{(-1)}\phi^{(0)} = \mathbf{L}^{(1)}\phi^{(-2)} + \mathbf{L}^{(0)}\phi^{(-1)} + \mathbf{L}^{(-1)}\phi^{(0)}.$$

Since $\mathbf{L}^{(1)} - \lambda^{(1)}\mathbf{1} = \mathbf{0}$ and since $\lambda^{(0)} = 0$,

$$\begin{pmatrix} c\partial_x & 0 \\ 0 & c\partial_x \end{pmatrix}\phi^{(-1)} = \begin{pmatrix} \lambda^{(-1)} + \frac{3Ti}{\pi} & \frac{3Ti}{\pi}(1+\eta) \\ \frac{3Ti}{\pi} & \lambda^{(-1)} + \frac{3Ti}{\pi}u \end{pmatrix}\phi^{(0)},$$

which is solvable by the Fredholm alternative, provided that

$$\det \begin{pmatrix} \lambda^{(-1)} + \frac{3Ti}{\pi}\bar{u} & \frac{3Ti}{\pi}(1+\bar{\eta}) \\ \frac{3Ti}{\pi} & \lambda^{(-1)} + \frac{3Ti}{\pi}\bar{u} \end{pmatrix} = 0,$$

where

$$\bar{\eta} = \frac{1}{T} \int_0^T \eta(x) \, dx \quad \text{and} \quad \bar{u} = \frac{1}{T} \int_0^T u(x) \, dx \quad (4.10)$$

are the means of η and u over the period. Therefore

$$\lambda^{(-1)} = -\frac{3Ti}{\pi} \bar{u} \pm \frac{3T}{\pi} \sqrt{-(1 + \bar{\eta})},$$

and if $1 + \bar{\eta} < 0$, so that $\text{Re}(\lambda^{(-1)}) \neq 0$, then the spectrum of (4.9) tends to infinity along some curve whose real part is nonzero.

Surprisingly,

$$1 + \bar{\eta} = \frac{4}{33}(2 + c^2) + \frac{1213}{1188}b_2, \quad (4.11)$$

not involving elliptic integrals, so that $1 + \bar{\eta} < 0$ when $b_2 < -\frac{288}{1213} \approx -0.2374$. For a proof of (4.11), see below.

We summarize our conclusion.

Theorem 5. *Let η and u denote a periodic traveling wave of (4.1), c the wave speed, and T the period, where c is in an interval of admissible wave speeds, depending on b_1 and b_2 . The spectrum of (4.9) satisfies*

$$\lambda = \frac{2\pi ic}{T}k + \left(-\frac{3Ti}{\pi} \bar{u} \pm \frac{3T}{\pi} \sqrt{-\frac{4}{33}(2 + c^2) - \frac{1213}{1188}b_2} \right) k^{-1} + O(k^{-2}) \quad \text{as } |k| \rightarrow \infty, \quad (4.12)$$

where \bar{u} is in (4.10). Particularly, if

$$b_2 < -\frac{144}{1213}(2 + c^2) \quad (4.13)$$

then the spectrum tends to infinity along some curve whose real part is nonzero.

We remark that \bar{u} can be expressed in terms of elliptic integrals. But we will not give details here because it does not influence the quantitative result.

Proof of (4.11). Integrating the second equation of (4.2) over the period, we arrive at

$$\int_0^T (1 + \eta(x)) \, dx = \int_0^T \left(1 + b_2 - \frac{1}{2}u^2 + cu \right) \, dx.$$

Recalling (4.4a), we rewrite

$$\int_0^T (1 + \eta(x)) \, dx = \oint_{\Gamma} \left(1 + b_2 - \frac{1}{2}u^2 + cu \right) \frac{du}{\sqrt{2Q(u)}}, \quad (4.14)$$

where Γ is a Jordan curve in the complex plane containing the range of $1 + \eta$, an interval of \mathbb{R} . Recalling (4.4b), moreover,

$$0 = \oint_{\Gamma} \frac{Q'(u) \, du}{\sqrt{2Q(u)}} = \oint_{\Gamma} \left(-\frac{9}{5c}u^2 + \frac{18}{5}u - \frac{144c^2 + 25b_2 - 900}{330c} \right) \frac{du}{\sqrt{2Q(u)}}. \quad (4.15)$$

Substituting (4.15) into (4.14), after some algebra we find

$$\int_0^T (1 + \eta(x)) \, dx = \oint_{\Gamma} \left(1 + b_2 + \frac{5}{18} \left(\frac{144c^2 + 25b_2 - 900}{330} \right) \right) \frac{du}{\sqrt{2Q(u)}}.$$

On the other hand,

$$T = \oint_{\Gamma} \frac{du}{\sqrt{2Q(u)}}.$$

Therefore

$$\frac{1}{T} \int_0^T (1 + \eta(x)) \, dx = 1 + b_2 + \frac{5}{18} \left(\frac{144c^2 + 25b_2 - 900}{330} \right) = \frac{4}{33}(2 + c^2) + \frac{1213}{1188}b_2.$$

This completes the proof. ■

4.3 Numerical experiments

Similarly as in Sections 2.3 and 3.3, we compute the spectrum of (4.9) numerically. When (4.13) holds true, we numerically evaluate (4.12) up to the order of k^{-1} .

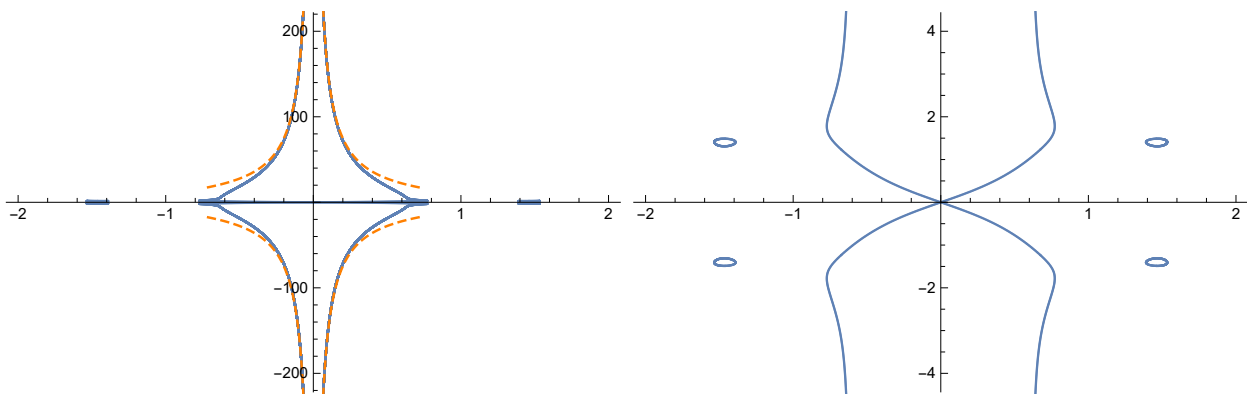


Figure 12: The numerically computed spectrum of (4.9) for $c = 3$, $b_1 = 0$, $b_2 = -2$, which satisfy (4.13). The spectrum tends towards infinity along the dashed curves $\pm 3.56k^{-1} \pm (4.25k - 18.43k^{-1})i$, $k \in \mathbb{R}$. On the right is a close-up for modulational instability near $0 \in \mathbb{C}$ and, additionally, four isolated and closed loops of the spectrum centered at $\approx \pm 1.47 \pm 1.39i$.

Figure 12 provides an example of the numerically computed spectrum of (4.9). Here b_1 and b_2 correspond to a bullet point in the region 4 of Figure 11, and c and b_2 satisfy (4.13). The spectrum tends towards infinity along the dashed curve, for which we evaluate (4.12) numerically up to the order of k^{-1} . Therefore the numerical result corroborates Theorem 5. The right panel shows modulational instability near $0 \in \mathbb{C}$ and, additionally, four isolated and closed loops of the spectrum whose real part is nonzero. Such closed loops of the spectrum are unusual, although isolated eigenvalues in the long wavelength limit, namely a solitary wave, can open up to a closed loop of spectrum for sufficiently large but finite wavelengths [16].

Figure 13 shows the spectrum of (4.9) for $b_1 = b_2 = 0$ in the region 4 of Figure 11, and $c = 4$ in an interval of admissible wave speeds, which do not satisfy (4.13). The right panel shows modulational and finite wavelength instability, but the spectrum lies along the imaginary axis otherwise, corroborating our analytical prediction.

Figures 14 and 15 show two examples of the spectrum, for which b_1 and b_2 are in the region 3 of Figure 11. In Figure 14, $b_1 = 15.97$ and $b_2 = 6.895$, for which the three intervals of admissible wave speeds are $(-\infty, -2.90)$, $(0.217, 0.802)$, $(2.23, \infty)$, and we take $c = 3$. Since $b_2 < 0$, (4.13) does not hold true. The numerically computed spectrum lies along the imaginary axis toward infinity. The right panel shows modulational and finite wavelength instability.

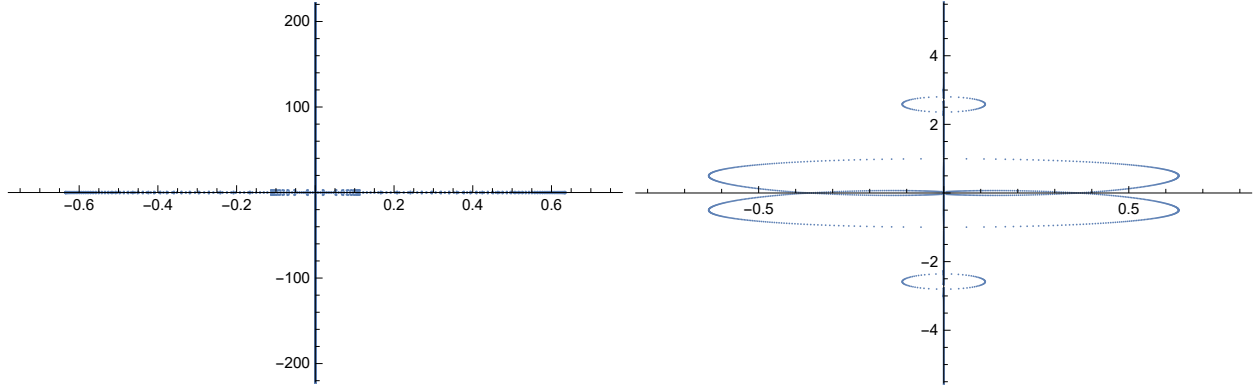


Figure 13: The spectrum of (4.9) for $c = 4$ and $b_1 = b_2 = 0$, which do not satisfy (4.13). The spectrum lies along the imaginary axis towards infinity. On the right is a close up for modulatory instability near $0 \in \mathbb{C}$ and finite wavelength instability near $\pm 2.6i$.

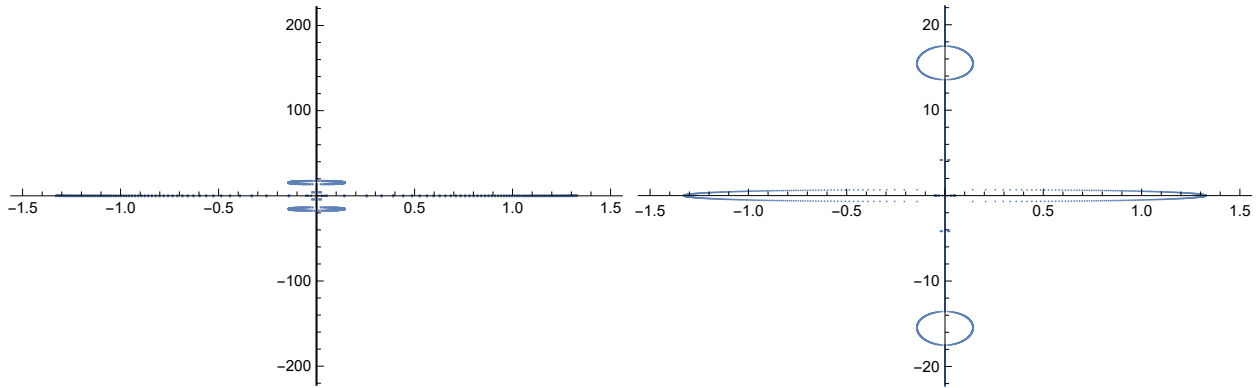


Figure 14: The spectrum for (4.9) for $c = 3$, $b_1 = 15.97$, $b_2 = 6.895$, which do not satisfy (4.13). The spectrum lies along the imaginary axis towards infinity. On the right is a close up for modulatory instability near $0 \in \mathbb{C}$ and, additionally, finite wavelength instability near $\pm 4.1i$ and $\pm 15.5i$, although the former is hard to distinguish.

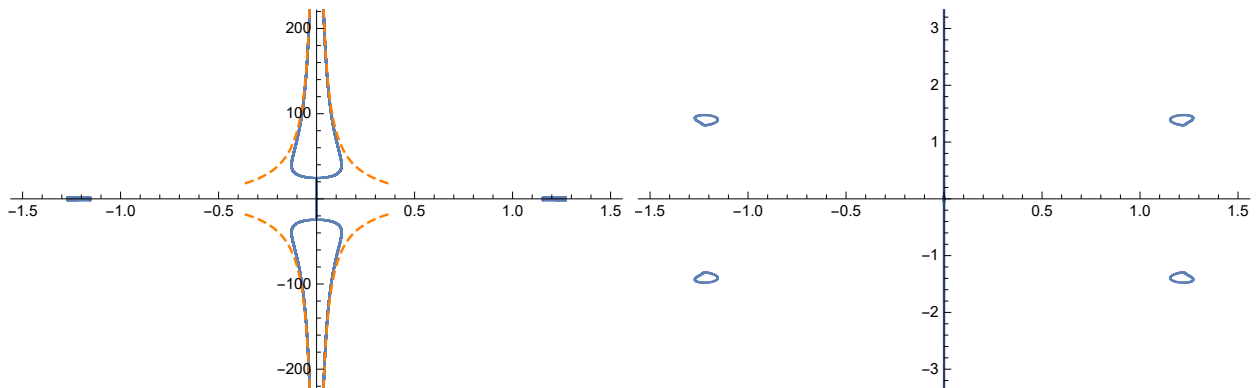


Figure 15: The spectrum of (4.9) for $c = 3$, $b_1 = 15.97$, $b_2 = -1.5$, which satisfy (4.13). The spectrum leaves the imaginary axis at $\approx \pm 24.5i$ and tends towards infinity along the dashed curves $\pm 1.80099k^{-1} \pm (4.44989k - 18.4791k^{-1})i$, $k \in \mathbb{R}$. On the right is a close up for no modulatory instability near $0 \in \mathbb{C}$, but rather four closed loops of the spectrum near $\pm 1.2 \pm 1.4i$.

In Figure 15, $b_1 = 15.97$ and $b_2 = -1.5$, for which the three intervals of admissible wave speeds are $(-\infty, -2.77)$, $(0.123, 1.03)$, $(1.95, \infty)$, and (4.13) holds true for $|c| \lesssim 3.26$. We take $c = 3$. The spectrum tends towards infinity along the dashed curve, for which we evaluate (4.12) numerically up to the order of k^{-1} . There is no modulational instability near $0 \in \mathbb{C}$ but four isolated and closed loops of the spectrum off the imaginary axis.

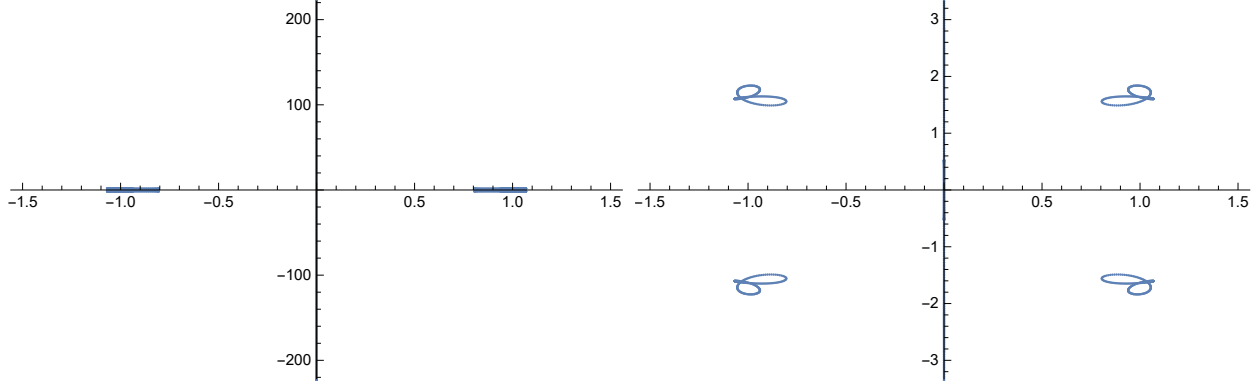


Figure 16: The spectrum of (4.9) for $b_1 = 15.97$, $b_2 = -1.5$, $c = 4$, which do not satisfy (4.13). The spectrum lies along the imaginary axis towards infinity. On the right is a close-up for no modulational instability near $0 \in \mathbb{C}$, but four isolated and closed loop of the spectrum off the imaginary axis.

Figure 16 shows the spectrum for $b_1 = 15.97$ and $b_2 = -1.5$, the same as in Figure 15, but $c = 4$, greater than Figure 15, for which (4.13) no longer holds true. The spectrum lies along the imaginary axis far away from $0 \in \mathbb{C}$. On the right is a close up for isolated and closed loops of the spectrum off the imaginary axis. There is no modulational instability.

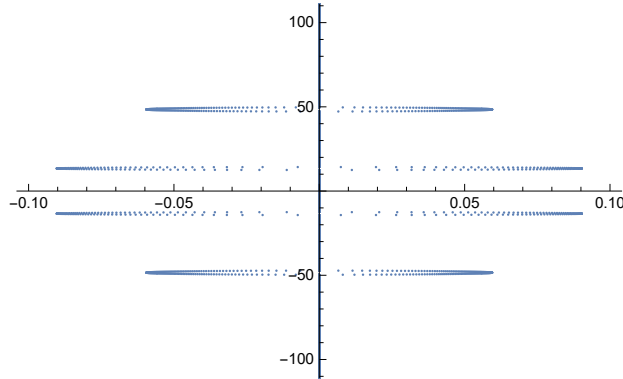


Figure 17: The spectrum of (4.9) for $c = 4$, $b_1 = 0$, $b_2 = 40$, which do not satisfy (4.13). The spectrum lies along the imaginary axis, other than finite wavelength instability near $\pm 12i$ and $\pm 50i$. Notice no modulational instability.

Last but not least, Figure 17 shows an example of the spectrum, for which the values of b_1 and b_2 correspond to the bullet point in the region 2 of Figure 11, and c and b_2 do not satisfy (4.13). The spectrum lies along the imaginary axis, other than finite wavelength instability. There is no modulational instability.

References

- [1] Jaime Angulo and Jose R. Quintero, *Existence and orbital stability of cnoidal waves for a 1D Boussinesq equation*, Int. J. Math. Math. Sci. (2007), Art. ID 52020, 36.
- [2] F. M. Arscott, *Periodic differential equations. An introduction to Mathieu, Lamé, and allied functions*, International Series of Monographs in Pure and Applied Mathematics, Vol. 66. A Pergamon Press Book, The Macmillan Co., New York, 1964.
- [3] T.B. Benjamin, J.L. Bona, and J.J. Mahony, *Model equations for long waves in nonlinear dispersive systems*, Philos. Trans. Roy. Soc. London Ser. A **272** (1972), 47–78.
- [4] D. J. Benney and J. C. Luke, *On the interactions of permanent waves of finite amplitude*, J. Math. and Phys. **43** (1964), 309–313.
- [5] J. L. Bona, M. Chen, and J.-C. Saut, *Boussinesq equations and other systems for small-amplitude long waves in nonlinear dispersive media. I. Derivation and linear theory*, J. Nonlinear Sci. **12** (2002), no. 4, 283–318.
- [6] ———, *Boussinesq equations and other systems for small-amplitude long waves in nonlinear dispersive media. II. The nonlinear theory*, Nonlinearity **17** (2004), no. 3, 925–952.
- [7] J. Boussinesq, *Théorie des ondes et des remous qui se propagent le long d'un canal rectangulaire horizontal, en communiquant au liquide contenu dans ce canal des vitesses sensiblement pareilles de la surface au fond*, J. Math. Pures Appl. (2) **17** (1872), 55–108.
- [8] Jared C Bronski, Vera Mikyoung Hur, and Mathew A Johnson, *Modulational instability in equations of KdV type*, New approaches to nonlinear waves, Springer, 2016, pp. 83–133.
- [9] Jared C. Bronski, Vera Mikyoung Hur, and Samuel Lee Wester, *Modulational instability for regularized long-wave models*, In preparation (2021).
- [10] Jared C Bronski and Mathew A Johnson, *The modulational instability for a generalized Korteweg–de Vries equation*, Archive for rational mechanics and analysis **197** (2010), no. 2, 357–400.
- [11] Jared C Bronski, Mathew A Johnson, and Todd Kapitula, *An index theorem for the stability of periodic travelling waves of Korteweg–de Vries type*, Proceedings. Section A, Mathematics-The Royal Society of Edinburgh **141** (2011), no. 6, 1141.
- [12] Hongqiu Chen, Min Chen, and Nghiem V. Nguyen, *Cnoidal wave solutions to Boussinesq systems*, Nonlinearity **20** (2007), no. 6, 1443–1461.
- [13] Min Chen, Christopher W. Curtis, Bernard Deconinck, Crystal W. Lee, and Nghiem Nguyen, *Spectral stability of stationary solutions of a Boussinesq system describing long waves in dispersive media*, SIAM J. Appl. Dyn. Syst. **9** (2010), no. 3, 999–1018.
- [14] Carmen Chicone, *Ordinary differential equations with applications*, Texts in Applied Mathematics, vol. 34, Springer-Verlag, New York, 1999.
- [15] M. S. P. Eastham, *The spectral theory of periodic differential equations*, Texts in Mathematics (Edinburgh), Scottish Academic Press, Edinburgh; Hafner Press, New York, 1973.

- [16] Robert A. Gardner, *Spectral analysis of long wavelength periodic waves and applications*, Journal für die reine und angewandte Mathematik **1997** (1997), no. 491, 149–182.
- [17] Vera Mikyoung Hur and Ashish Kumar Pandey, *Modulational instability in nonlinear nonlocal equations of regularized long wave type*, Phys. D **325** (2016), 98–112.
- [18] Avinash Khare and Uday Sukhatme, *New solvable and quasiexactly solvable periodic potentials*, Journal of Mathematical Physics **40** (1999), no. 11, 5473–5494.
- [19] Ayşe Kiper, *Fourier series coefficients for powers of the Jacobian elliptic functions*, Mathematics of Computation **43** (1984), no. 167, 247–259.
- [20] D. J. Korteweg and G. de Vries, *On the change of form of long waves advancing in a rectangular canal, and on a new type of long stationary waves*, Philos. Mag. (5) **39** (1895), no. 240, 422–443.
- [21] Wilhelm Magnus and Stanley Winkler, *Hill’s equation*, Dover Publications, Inc., New York, 1979, Corrected reprint of the 1966 edition.
- [22] Georgios Pastras, *The Weierstrass elliptic function and applications in classical and quantum mechanics*, SpringerBriefs in Physics, Springer, Cham, [2020] ©2020, A primer for advanced undergraduates.
- [23] Robert L Pego and José Raúl Quintero, *Two-dimensional solitary waves for a benney–luke equation*, Physica D: Nonlinear Phenomena **132** (1999), no. 4, 476–496.
- [24] G. B. Whitham, *Linear and nonlinear waves*, Pure and Applied Mathematics (New York), John Wiley & Sons, Inc., New York, 1999, Reprint of the 1974 original, A Wiley-Interscience Publication.
- [25] E. T. Whittaker and G. N. Watson, *A course of modern analysis*, 1996, An introduction to the general theory of infinite processes and of analytic functions; with an account of the principal transcendental functions, Reprint of the fourth (1927) edition, pp. vi+608.

A The spectrum for the generalized KdV equation

Let $\theta \in [0, 1]$ and we consider the spectral problem

$$\lambda\phi = \phi_{xxx} - c\phi_x + \theta(u(x)\phi)_x, \quad \phi \in L^2(\mathbb{R}/2\pi\mathbb{Z}), \quad (\text{A.1})$$

for some smooth and 2π periodic function u for some $c \neq -1, \in \mathbb{R}$. We wish to show that the spectrum of (A.1) lies in the imaginary axis outside some bounded set. Let

$$\phi(x) = \sum_{k \in \mathbb{Z}} \hat{\phi}_k e^{ikx} \quad \text{and} \quad u(x) = \sum_{k \in \mathbb{Z}} \hat{u}_k e^{ikx},$$

and we can reformulate (A.1) equivalently as

$$\hat{\phi}_k + \frac{i\theta k}{\lambda + ik^3 + ick} \sum_{n \in \mathbb{Z}} \hat{u}_n \hat{\phi}_{n-k} = 0, \quad k \in \mathbb{Z}. \quad (\text{A.2})$$

Let

$$S_k = \left\{ \lambda : |\lambda + ik^3 + ick| \leq k \sum_{n \in \mathbb{Z}} |\hat{u}_n| \right\} \quad \text{and} \quad S = \bigcup_{k \in \mathbb{Z}} S_k.$$

We pause to remark that $\sum_{n \in \mathbb{Z}} |\hat{u}_n| < +\infty$ because u is smooth, whence $|\hat{u}_n| \rightarrow 0$ as $|n| \rightarrow \infty$ more rapidly than polynomially. Observe that:

- The spectrum of (A.1) is contained in S because if $\lambda \notin S$ then (A.2) is invertible of $\widehat{\phi}_k$ for any $k \in \mathbb{Z}$ for any $\theta \in [0, 1]$;
- S_k are disjoint when $|k| \gg 1$ because $|\omega(k+1) - \omega(k)| \rightarrow \infty$ as $|k| \rightarrow \infty$, where $\omega(k) = -k^3 - ck$ is the dispersion relation of (A.1); For a regularized long-wave model, such as (1.3), on the other hand, $|\omega(k+1) - \omega(k)|$ remains bounded for all $k \in \mathbb{R}$;
- λ is continuous in $\theta \in [0, 1]$ and there is one in each S_k when $\theta = 0$, whereby there is exactly one in each S_k when $\theta = 1$.

To recapitulate, there are countably many S_k outside of a bounded set, each of which contains one eigenvalue of (A.1). Since (A.1) remains invariant under

$$\lambda \mapsto \lambda^* \quad \text{and} \quad \phi \mapsto \phi^*$$

where the asterisk denotes complex conjugation, and under

$$\lambda \mapsto -\lambda \quad \text{and} \quad x \mapsto -x,$$

if there is one eigenvalue in each S_k then such an eigenvalue must lie in the imaginary axis. Therefore only finitely many eigenvalues can fall off the imaginary axis. The same will hold true for the quasi-periodic boundary condition.